KARADENİZ TECHNICAL UNIVERSITY
THE GRADUATE SCHOOL OF NATURAL AND APPLIED SCIENCES

DEPARTMENT OF FOREST ENGINEERING

ANALYSIS OF WILDFIRE DYNAMICS IN THE HIMALAYAN REGION (2016-2025) USING REMOTE SENSING AND GEOGRAPHIC INFORMATION SYSTEMS

MASTER'S THESIS

ZARAK KHAN AFRIDI

DECEMBER 2025
TRABZON

KARADENİZ TECHNICAL UNIVERSITY
THE GRADUATE SCHOOL OF NATURAL AND APPLIED SCIENCES

DEPARTMENT OF FOREST ENGINEERING

ANALYSIS OF WILDFIRE DYNAMICS IN THE HIMALAYAN REGION (2016-2025) USING REMOTE SENSING AND GEOGRAPHIC INFORMATION SYSTEMS

ZARAK KHAN AFRIDI
ORCID :

This thesis is accepted to give the degree of
"MASTER OF SCIENCE"
By
The Graduate School of Natural and Applied Sciences at
Karadeniz Technical University

The Date of Submission : 11 / 11 /2025
The Date of Examination : 09 / 12 /2025

Supervisor : Doç. Dr. Kadir Alperen COŞKUNER
ORCID : - - -

Trabzon 2025

KARADENİZ TECHNICAL UNIVERSITY
THE GRADUATE SCHOOL OF NATURAL AND APPLIED SCIENCES

DEPARTMENT OF FOREST ENGINEERING
ZARAK KHAN AFRIDI

ANALYSIS OF WILDFIRE DYNAMICS IN THE HIMALAYAN REGION (2016-2025) USING REMOTE SENSING AND GEOGRAPHIC INFORMATION SYSTEMS

Has been accepted as a thesis of

MASTER OF SCIENCE

after the Examination by the Jury Assigned by the Administrative Board of the Graduate School of Natural and Applied Sciences with the Decision Number 2129 dated 20 / 11 / 2025

Approved By

Chairman : Prof. Dr. Ertuğrul BİLGİLİ

Member : Prof. Dr. Bülent SAĞLAM

Member : Doç. Dr. Kadir Alperen COŞKUNER

Prof. Dr. Asim KADIOĞLU
Director of Graduate School

FOREWORD

The Erasmus Mundus MEDfOR Program, which was funded by the European Union's Erasmus+ Program, served as the framework for the conduct of this study. The University of Lisbon's Instituto de Agronomia managed the program's coordination. I would like to express my profound gratitude to the MEDfOR Secretariat and the European Union's Erasmus+ Program for their kind financial support, as well as to all of the host universities that took me in during my entire study.

I would like to thank to certain people for their tremendous help during my thesis as MEDfOR. This thesis would not be possible without help of my Supervisor, Assoc. Prof. Dr. Kadir Alperen COSKUNER, who helped me in a very critical time and guided me to a right path. I would also like to thanks to Prof. Ertugrul BILGILI, who accepted me to do my master’s research at Karadeniz Technical University.

Beside that, I want to thanks all my friends, classmates and my professors at University of Padua and at University of Lleida. My special thanks is for my family, even though they were far away from me, they showed true love and support during my studies.

Zarak Khan AFRIDI

Trabzon 2025

THESIS STATEMENT

I hereby declare that I have completed this study titled "Analysis of Wildfire Dynamics in the Himalayan Region (2016–2025) Using Remote Sensing and Geographic Information Systems", which I have submitted as my Master's Thesis, from beginning to end under the responsibility of my advisor and mentor Assoc. Prof. Kadir Alperen COŞKUNER. I have downloaded the data myself from different NASA FIRMS, Copernicus Data Space Ecosystem and Climate data store. I have performed the analyses that I have fully indicated the information I have received from other sources in the text and bibliography, that I have acted in accordance with scientific research and ethical rules throughout the study process, and that I accept all legal consequences in case the contrary occurs. 09 / 12 / 2025

Zarak Khan AFRIDI

TABLE OF CONTENT

Page No

Master's Thesis

SUMMARY

ANALYSIS OF WILDFIRE DYNAMICS IN THE HIMALAYAN REGION USING REMOTE SENSING AND GEOGRAPHIC INFORMATION SYSTEMS

Zarak Khan AFRIDI

Karadeniz Technical University
The Graduate School of Natural and Applied Sciences
Forest Engineering Graduate Program
Supervisor: Assoc. Prof. Kadir Alperen COŞKUNER
2025, 68 Pages

This study examines the behavior of wildfires using the WFA Pocket Simulator across eight distinct events occurring throughout the Himalayan region, including Nepal, India, Bhutan, Pakistan, and Tibet. By utilizing VIIRS active fire data along with Sentinel-2 L2A imagery sourced from the Copernicus Data Space Ecosystem, we derived the Normalized Burn Ratio (NBR) and its differenced form (dNBR) to quantify the conditions before and after the fires and to outline the burned areas at a spatial resolution of 20 meters. From this data, the rate of spread (ROS) and the burned area were calculated for each individual fire. To provide context for how the fires spread, additional meteorological parameters such as air temperature, wind speed and direction, and relative humidity were sourced from ERA5's post-processed daily statistics. The model's performance was evaluated by comparing the simulated Rate of Spread (ROS) and burned area values to those observed, using bias and an adjusted coefficient of determination (R^2). The results showed consistently low R^2 values, indicating a weak statistical correlation between the simulations and what was actually observed for all the fires. Overall, this study highlights how important local calibration and multi-parameter validation are when simulating wildfires in hilly regions.

Keywords: Fire behavior, Himalayan region, Remote sensing, Wildfire

Yüksek Lisans Tezi

ÖZET

HİMALAYA BÖLGESİNDE ORMAN YANGINI DİNAMİKLERİNİN (2016-2025) UZAKTAN ALGILAMA VE COĞRAFİ BİLGİ SİSTEMLERİ İLE ANALİZİ

Zarak Khan AFRIDI

Karadeniz Teknik Üniversitesi
Fen Bilimleri Enstitüsü
Orman Mühendisliği Anabilim Dalı
Danışman: Doç. Dr. Kadir Alperen COŞKUNER
2025, 68 Sayfa

Bu çalışma, Nepal, Hindistan, Butan, Pakistan ve Tibet dahil olmak üzere Himalayalar bölgesinde meydana gelen sekiz farklı olayda WFA Cep Simülatörü kullanılarak orman yangınlarının davranışını incelemektedir. Copernicus Veri Alanı Ekosisteminden elde edilen Sentinel-2 L2A görüntüleriyle birlikte VIIRS aktif yangın verilerini kullanarak, yangınlardan önceki ve sonraki koşulları ölçmek ve yanmış alanları 20 metrelik bir mekansal çözünürlükte özetlemek için Normalleştirilmiş Yanma Oranı'nı (NBR) ve farklılaştırılmış formunu (dNBR) analiz edildi. Bu verilerden, her bir yangın için yayılma oranı (ROS) ve yanan alan hesabı yapıldı. Yangın davranışı ve hava halleri arasındaki ilişkinin analizi için, hava sıcaklığı, rüzgar hızı ve yönü ve bağıl nem gibi ek meteorolojik parametreler, ERA5'in sonradan işlenmiş günlük istatistiklerinden elde edilerek analiz edildi. Modelin performansı, simüle edilen Yayılma Oranı (ROS) ve yanmış alan değerleri belirleme katsayısı (R^2) kullanılarak gözlemlenen değerlerle karşılaştırılmasıyla değerlendirildi. Analiz sonucunda Yanan alan ve ROS tahmininde düşük R^2 değerleri elde edildi. Bu durum VFA simülatorü ile gerçekte gözlemlenen ROS ve yanan alan arasında zayıf bir istatistiksel ilişki olduğunu gösterdi. Genel olarak, bu çalışma, engebeli bölgelerdeki orman yangınlarını simüle ederken yerel kalibrasyonun ve çok parametreli doğrulamanın önemli olduğunu vurgulamaktadır.

Anahtar Kelimeler: Yangın davranışı, Himalaya bölgesi, Uzaktan algılama, Orman yangını

LIST OF FIGURES

Page No

LIST OF TABLES

Page No

ACRONYMS AND ABBREVIATIONS

dNBR	: Diffrenced Normalized Burn Ratio
EVI	: Enhanced Vegetation Index
FHY	: First - half year
GIS	: Geographic Information Systems
GS	: Growing season
MODIS	: Moderate Resolution Imaging Spectroradiometer
NDVI	: Normalized Difference Vegetation Index
NDMI	: Normalized Difference Moisture Index
NBR	: Normalized Burn Ratio
PVR	: Post-fire vegetation recovery
PREC	: Precipitation
RS	: Remote Sensing
ROS	: Rate of spread
RH	: Relative humidity
T	: Temperature
VIIRS	: Visible Infrared Imaging Radiometer Suite
WFA Pocket	: Wildfire Analyst Pocket

1. GENERAL INFORMATION

1.1. Introduction

Although forests cover nearly one-third of the Earth's surface and are essential for preserving biodiversity, providing ecosystem services, and supporting human well-being, they are also highly susceptible to fires that destroy millions of hectares of forest each year (Brandon, 2014). Fires have a significant impact on forest ecosystems, forming them fundamentally (McLauchlan et al., 2020). However, human activity has significantly changed the global fire regime, making various ecosystems more susceptible (Bowman et al., 2011). Fire incidents are expected to rise by roughly 27% worldwide by 2050 compared to 2000 levels (Robinne et al., 2018). Forest fires, often referred to as unwanted wildfires, demonstrate a significant environmental challenge in today's world. These fires have potential to influence the structure, distribution and composition of vegetation across various environments. It is estimated that each year, forest fires affect more than 350 million hectares of land worldwide (Jakhar et al., 2023).

The Himalayan Mountain range is one of the most prominent and ecologically significant landscapes in the world, stretching over 2,400 kilometers across five countries: Nepal, India, Bhutan, China, and Pakistan (Pathak et al., 2023). This region supports a remarkable diversity of ecosystems, ranging from subtropical forests in the lower foothills to alpine meadows and snow-covered peaks at higher elevations. These diverse ecosystems harbor a wealth of biodiversity, including numerous endemic plant and animal species, many of which are globally threatened (Pathak et al., 2023).

The forests of the Himalayas are vital not only for biodiversity conservation but also for maintaining regional hydrological cycles. They play a critical role in regulating water supply by feeding numerous rivers and streams that sustain millions of people downstream. Additionally, Himalayan forests provide essential ecosystem services such as carbon sequestration, soil conservation, and climate regulation, contributing to both local livelihoods and global environmental health (Lepcha et al., 2021).

However, this ecologically sensitive region faces multiple environmental threats, among which forest fires are increasingly prominent. Forest fires have historically been a natural part of many forest ecosystems, contributing to nutrient recycling, seed germination, and maintenance of plant diversity (Raison et al., 2009). Yet, the frequency, intensity, and extent of fires have escalated in recent decades, driven by a combination of climatic changes, human activities, and land-use modifications (Raison et al., 2009).

Climate change has altered temperature and precipitation regimes in the Himalayas, leading to warmer and drier conditions, especially during pre-monsoon seasons. These climatic shifts create favorable conditions for increased fire incidence and severity (Adhikari et al., 2021). At the same time, anthropogenic factors such as forest clearing, agricultural expansion, grazing, and unsustainable forest management practices contribute to changing fire regimes (Shlisky et al., 2009). Additionally, increased human encroachment and infrastructure development have heightened the risk of accidental or intentional fires (Naser & Kodur, 2025).

The consequences of escalating forest fires in the Himalayas are profound. Apart from the direct loss of forest cover and biodiversity, fires exacerbate soil erosion, reduce water quality, and release significant amounts of greenhouse gases (Mandal & Banik, 2025). They also threaten the socio-economic fabric of rural mountain communities that depend on forest resources for fuel, fodder, and non-timber products (Masoodi & Sundriyal, 2020).

Despite the growing significance of forest fires in the region, systematic studies on fire behavior and regimes in the Himalayas remain scarce, largely due to the region's complex topography, political boundaries, and data limitations. Advances in remote sensing technologies and climate modeling offer new opportunities to fill these gaps by providing detailed spatiotemporal fire data and enabling predictive modeling (Shekede et al., 2024).

The frequency and intensity of wildfires in the Himalayan region have been rising because of fuel accumulation, shifting land use, and climate unpredictability. However, the area is still poorly researched and has a lack of data when compared to North America, Europe, or Australia (S. W. Wang et al., 2021).

WFA Pocket Simulator was introduced by Technosylva S.L. that provides real time fire behavior analysis, prediction and helps fire analyst and Inspectors to deploy field crew on the fire incident area. It is a mobile modelling tool that integrates several parameters like fuel type, wind direction/speed, aspect/slope ratio, live and dead fuel moisture and calculate the outputs like rate of spread (ROS), flame length, fire perimeter and burned area. WFA pocket integrates real time weather, fuel assimilation and GIS data, that makes it acceptable for firefighters for rapid initial attack or field assessments during a fire. Moreover, it can be used both online and offline, helping decision making during fire emergencies and to allocate resources to the area.

Rapid fire behavior forecasts are possible with fire modeling tools like the WFA Pocket Simulator; however, they were created in environments with flat or rolling terrain, well-characterized meteorological, and relatively homogeneous fuels. WFA Pocket is a fire behavior modelling tool built for firefighters and fire analyst for field deployment. This tool incorporates Fuel type, rate of spread (ROS), wind and speed direction, slope and aspect of the incident area, live and dead fuel moisture to estimate total burnt area during the fire incident. The Himalayas' varied terrain, diverse vegetation, and distinct microclimates may cause these models to perform poorly. Due to a lack of rigorous validation, decision-makers are unsure if outputs (burned area, rate of spread) are dependable enough for operational usage.

The primary objective of this study is to critically assess the ability of the WFA Pocket Simulator to predict wildfire dynamics and behavior across multiple case studies of Himalayan fires, with a particular focus on burned area and rate of spread (ROS). Specifically, this research aims to evaluate how accurately the simulator can replicate observed burned area and ROS across different fire events, quantify any systematic bias in its predictions, and assess the explanatory power of the simulator using statistical measures such as R^2 and Adjusted R^2. Additionally, the study investigates how the operational application of WFA Pocket in the Himalayan environment may be influenced by model bias and limitations in statistical fit. By addressing these questions, the thesis examines both the physical behavior of individual fires and the broader patterns and drivers of wildfire dynamics in complex mountainous landscapes.

1.2. Literature Review

1.2.1. Wildfires in the Himalayan Region

Forest fires have emerged as a significant ecological and socio-economic concern in the Himalayan region during the past decade (S. W. Wang et al., 2021). The complex topography, diverse forest types, and varying climatic conditions make the Himalayas particularly vulnerable to wildfires which are increasingly frequent and intense due to climate change and anthropogenic pressures (Bhujel et al., 2022). This section reviews notable forest fire incidents across Nepal, India, Bhutan, Pakistan, and China from 2016 to 2025, highlighting spatial and temporal trends and underlying drivers.

- Wildfires in Nepal (2016-2025)

One of the main causes of Nepal's forest deterioration is wildfire (Fig.1). With 89% of them happening in March, April, and May, most forest fires are caused by humans and happen during the dry season (Matin et al., 2017). Every year, 400,000 hectares of land are burned by forest fires in Nepal (Bajracharya, 2002). Forest fires destroy the Terai, Siwalik, and mid-hills' tropical, subtropical, and temperate forests every year, especially areas with a high distribution of *Shorea robusta* and *Pinus roxburghii*. These areas have a high frequency of forest fires, primarily due to the hot, dry weather and the proximity of the forests to roads, agricultural land, and human populations. Of all forest fire incidents, 58% are caused by intentional burning by grazers, poachers, and collectors of non-timber forest products, 22% are the result of carelessness, and 20% are the result of accidents (Kunwar & Khaling, 2006). Temperatures in Nepal's Terai and mid-hill regions are steadily rising because of climate change. Over the past few decades, summer temperatures in this area have risen by 38°C, and by 2030, 2060, and 2090, they are predicted to rise by 1.48°C, 2.88°C, and 4.78°C. Forest fires are predicted to rise in Nepal in the upcoming years due to changes in the country's temperature and precipitation patterns (Matin et al., 2017).

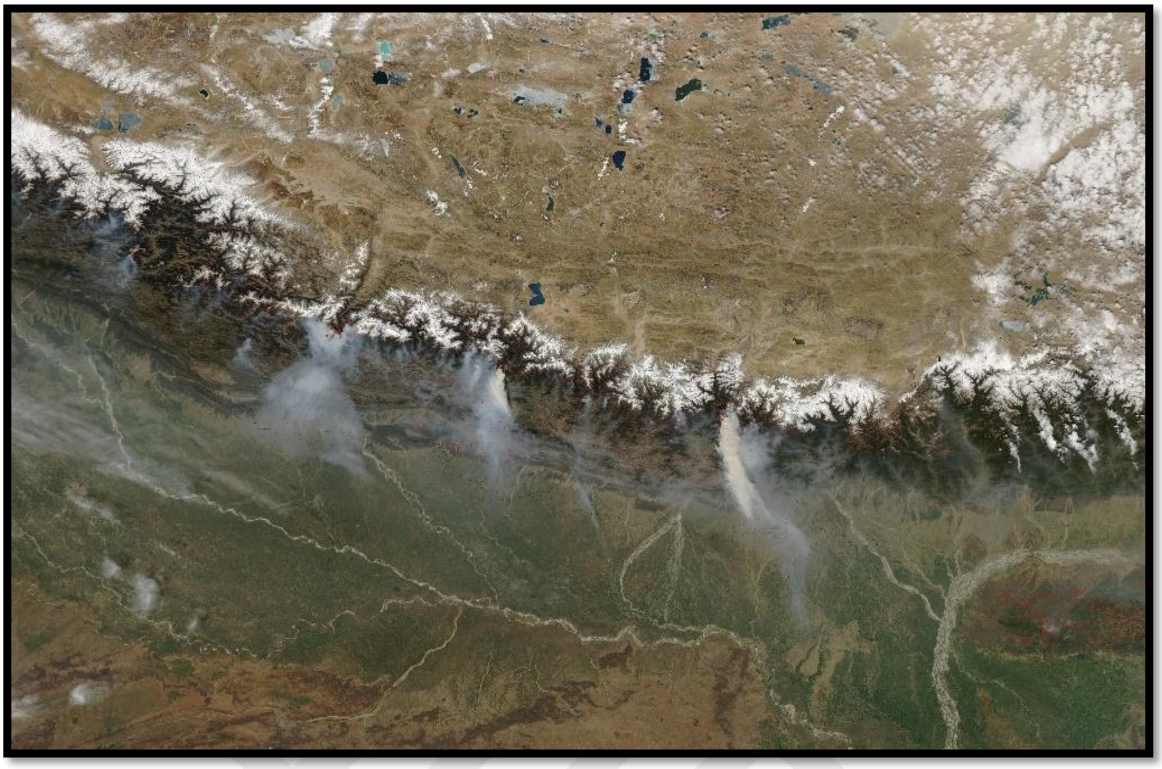

Figure 1. The MODIS satellite image, taken on March 12, 2009, depicts extensive forest fires in Nepal's Himalayan area (Matin et al., 2017).

Nepal suffers ecologically and even economically from forest fires, particularly during the country's protracted and arid summers. Since the 2016 forest fires burned 13,000 square kilometers and are said to have killed 15 people, they also represent a major threat to life and property in the nation (Babar Mahal, 2012). There were 121 forest fires in total in 2016. Very few fires occurred on slopes lower than 5%, whereas the maximum number of fire events were documented at elevations greater than 35 degrees. Approximately 106 fires were reported in areas with temperatures higher than 33 °C (Joshi et al., 2024). The year 2016 had the greatest fire point, followed by 2021 and 2019 (Joshi et al., 2024). In 2016, forest fires destroyed about 12,000 community woods across 50 districts in Nepal, resulting in 15 fatalities. In January 2020, there were just 17 forest fire incidences, compared to 56 in 2019, 76 in 2018, and 29 in 2017 (Hameed, 2024). In 2018, the largest recorded burned area was 4729.72 hectares, and in 2017, 4575.391 hectares was the smallest burned area ever measured.

In 2021 alone, Nepal experienced around 6,000 forest fires between January and July (Jadhav, 2025). Lumbini's forests have been impacted by flames on 11,448 hectares. There were around 5,000 fires throughout the countryside last year, 2024. In Nepal, the number of forest fires has significantly increased, with over 300 occurrences being documented in the first two months of 2025 (Thapa et al., 2025). The forecast indicated that, under three specific assumptions: business as usual, risk of doubling, and risk of tripling, the anticipated burned area was likely to increase in 2050, 2080, and 2100 (Badal & Mandal, 2021).

- Wildfires in India (2016-2025)

The Indian Himalayan states, particularly Uttarakhand, Himachal Pradesh, and Sikkim, have witnessed severe fire incidents within the 2016-2025 period. In May and June of 2016, forest fires destroyed about 3774.14 km2 (15.28%) of Uttarakhand's total forest cover. Tehri Garhwal, Pauri Garhwal, and Nainital districts were the most severely damaged.

India's overall forest cover, which encompasses 18 different forest types, is around 76.4 million hectares (22% of India's total land and 2% of the world's total wooded area, which includes 1% of the world's primary forest). Notably, the 2016 forest fires in Uttarakhand led to extensive damage across over 4,500 hectares of forest land, with satellite imagery indicating widespread hotspots (Tiwari et al., 2024). Nonetheless, in 2017, the district of Nainital had the most forest fires (411), while the district of Rudraprayag recorded the fewest forest fires. The district of Tehri Garhwal had the most forest fires in 2019 (8555), while the district of Rudraprayag had the fewest (39) (Mina et al., 2023). In May 2019, there were 192 active forest fires reported in India, with the highest number occurring in Uttarakhand (91), Chhattisgarh (36), and Madhya Pradesh (17).

More than 30,000 forest fires occurred in India in 2019, according to MODIS data and additionally, it was shown that human activity was responsible for about 95% of India's forest fires (Badal & Mandal, 2021).

Similar fire peaks occurred in 2019 and 2021, when dry weather and unregulated human activities such as illegal fuelwood collection and religious fire rituals increased fire susceptibility (P. Singh et al., 2021). Fire incidents in these regions have often been linked to warming trends and shifting precipitation patterns, aligning with broader regional climate change impacts (Batllori et al., 2013). Post-fire assessments revealed significant loss of biodiversity and increased soil erosion, threatening the fragile mountain ecosystems (Scott et al., 2009). According to the ISFR report from 2021, there were 345,989 forest fires in the country between November 2020 and June 2021, which is a clear rise from the 87,509 that were documented during the same period 2018-2019. This is the nation's second-highest number of forest fire reports.

Similarly, between January 1 and March 31, 2022, there were 136,604 fire points nationwide (Priya et al., 2024). During the summer (March to June) of 2022, quick field visits were made to ten forest fire-affected regions in the districts of Pauri, Tehri, and Chamoli in addition to secondary data sources. In 2022, 3425 hectares of land were affected by forest fires. The district of Almora had the largest impacted area (904 ha), followed by the districts of Pauri (691 ha) and Pithoragarh (316 ha). Tehri (247 ha), Bageshwar (237 ha), Haridwar (215 ha), and Uttarkashi (203 ha) were among the other districts where forest fires had destroyed more than 200 hectares of land. There were between 100 and 200 hectares of forest fire-affected land in the districts of Chamoli, Rudraprayag, and Nainital. Champawat (52 ha), Dehradun (87 ha), and the USN district had the smallest impacted area (2 ha). At almost 124,000 USD, 2021 had the largest economic loss during this time, with 2018 coming in second. At about $4000 USD, 2020 observed the least amount of economic damage (Sati 2024). Between November 2023 and June 2024, 10,136 fire incidents were reported in Himachal Pradesh. Telangana (3,983.28 km2), Chhattisgarh (3,812.28 km2), Madhya Pradesh (3,172.13 km2), Maharashtra (4,095.04 km2), and Andhra Pradesh (5,286.76 km2) are the top 5 states with the highest burnt areas. Goa (0.45 km2), Sikkim (2.08 km2), Haryana (44.63 km2), and Punjab (40.55 km2), on the other hand, reported comparatively few burned areas (KUMAR, 2000).

- Wildfires in Bhutan (2016-2025)

Bhutan is a tiny landlocked nation on the southern slope of the Eastern Himalayas that covers 3,839,400 hectares. The first forest fire devastated about 8 hectares of forest area in Sangaygang on February 12 at around 12 p.m. A smaller fire that broke out at Wangchuck Resort in Taba at around 3 p.m. was put out with the assistance of volunteers. Over Samarzingkha, another large fire on February 13, 2016, damaged about 15 hectares of plantation and surrounding forest. In Bhutan, forest fire incidents and damage grew from 40 occurrences in 2019 that destroyed 352.72 hectares to 43 cases that destroyed 4308.05 hectares in 2021 alone, according to (Tshering et al., 2020). About 50 forest fire occurrences were reported by the DoFPS during the peak fire season, which ran from November 2024 to March 2025, resulting in the destruction of an estimated 12,000 acres of forest. A total of 261 forest fire occurrences has burned about 70,696 acres of forest nationwide throughout the last five years (2020-2024). In contrast, in 2021 Bhutan had only 194 active fires over that time. Bhutan experienced just 110 forest fire events over the research period (Gurung et al., 2023).

- Wildfires in Pakistan (2016-2025)

In Pakistan, forest fires have increased in frequency, especially during the summer months of May through July in the northern coniferous and scrub forests. Between 2016 and 2025, Pakistan experienced a noticeable increase in the frequency and severity of forest fires, particularly in ecologically sensitive regions such as the Himalayan foothills, Margalla Hills, Balochistan's juniper forests, and northern areas including Chitral and Swat (Rafaqat, Iqbal, Kanwal, & Weiguo, 2022). This rise has been attributed to a combination of anthropogenic activities and climate change, with prolonged dry seasons, rising temperatures, and human negligence such as campfires and slash-and-burn agriculture acting as key drivers (Rafaqat, Iqbal, Kanwal, & Song, 2022).

Consolidated data from the Daily Situation Reports (DSR) published by the department of forestry, environment, and wildlife in Khyber Pakhtunkhwa indicates that between May 23 and June 13, 2022, 283 fire events were registered throughout the province. The Forest Department reports that fires destroyed 1,392.5 hectares in 2016-17, 1,668.42 hectares in 2017-18, 1,252.12 hectares in 2018-19, 1,220.65 hectares in 2019-20, and 1,033.54 hectares throughout 2020-21 (Nafees et al., 2024). Between July 2018 and June 2019, there were numerous forest fire occurrences in Pakistan's northwest Khyber Pakhtunkhwa province, resulting in the loss of about 1.2 million trees (Badal & Mandal, 2021).

For example, in May 2016, eight distinct forest fire occurrences occurred on the Margalla Hills near Islamabad in 15 days, resulting in substantial environmental damage (Tariq et al., 2021). For example, the wildfires in Khyber Pakhtunkhwa's Swat Valley in 2019 devastated more than 50,000 acres of forest, affecting wildlife habitats and putting species like the Markhor goat and Himalayan brown bear in jeopardy (Tariq et al., 2020). The anticipated damage from the Chitral fires in 2020 exceeded PKR 100 million (USD 600,000), including livestock losses and infrastructure damage (Kausar et al., 2025).

Notably, the year 2022 saw a catastrophic fire in the Sherani Forest of Balochistan, which severely damaged centuries-old juniper trees, while hundreds of smaller fires were reported across Khyber Pakhtunkhwa. Pakistan's susceptibility to natural disasters such as wildfires is further highlighted by the 2023 wildfire (or related disaster) that happened in

Balochistan's Hingol National Park (Accountability Lab Pakistan 2025). The Margalla Hills National Park has also faced recurrent fires, often suspected to be deliberate, highlighting the need for improved monitoring and enforcement mechanisms (Tariq et al., 2020).

In May 2024, a wildfire started in Islamabad's Margalla Hills National Park because of an extreme heat wave. This was another significant event. It took the efforts of more than 75 firemen to contain the fire, which caused significant damage. Furthermore, there has been a concerning rise in forest fires in Khyber Pakhtunkhwa, with 306 occurrences reported in the first half of this year. With 122 occurrences, Abbottabad was the most severely affected. Forest fires in Punjab increased dramatically in 2024 because of human activities and climate change. Compared to 199 events in 2023, 377 incidents had been registered by June, an 89% increase. There were 152 fires in May alone, with the most impacted locations (Tariq et al., 2021).

Remote sensing data from MODIS and VIIRS have consistently shown increasing hotspots and burned area across Pakistan during the peak fire months of May to July, suggesting an ongoing and intensifying pattern (NASA FIRMS, 2025). Despite efforts by local forest departments and the National Disaster Management Authority, the effectiveness of fire prevention and control remains limited due to resource constraints and lack of community engagement.

- Wildfires in China (2016-2025)

The frequency and intensity of forest fires in China significantly decreased between 2016 and 2025, a development that was mostly ascribed to improved preventative techniques and fire management regulations (Jingjing et al., 2025). Due to dry weather and strong winds, the May 2, 2017, forest fire in Inner Mongolia's Greater Hinggan Mountains spread quickly, endangering significant forest resources across vast areas. With the help of hundreds of fire engines and 12 aircraft, about 8,300 firefighters were called in to put out the fire (Y. Yang et al., 2021). 30 people, including 27 firemen and three local citizens, were killed in a devastating forest fire in Muli County, Sichuan Province, China, in March 2019 (Lian et al., 2024). A severe forest fire in Xichang, Sichuan Province, China, in March 2020 claimed the lives of one forestry guide and eighteen firemen. Around 3 p.m. local time on March 30, the fire broke out, endangering the city's safety (Lu et al., 2024). In August 2022, there were forest fires in Chongqing, China (Li et al., 2025).

A large forest fire broke out on March 17, 2024, close to Baizi village in Yajiang County, Sichuan province, and quickly spread over mountain ridges because of unexpected gusty winds (Y. Yang et al., 2021). A major forest fire outbreak occurred in Jilin Province, China, in March 2024, scorching roughly 19,594 hectares of land between March 12 and March 15. Although no fatalities were reported, the Global Disaster Alert and Coordination System estimates that 3,549 persons were impacted by the fire within its perimeter. The incident was deemed to have no humanitarian significance. However, more flames broke out in other regions of China, such as the provinces of Yunnan and Sichuan, over the same time frame. At least four people were killed by wildfires in these southern areas, including in Lincang and Wenshan in Yunnan, while about 4,900 people were evacuated from Yajiang County in Sichuan. These occurrences highlight the area's susceptibility to wildfire outbreaks, especially in the arid spring and under variable (Kejun, 2020).

Four people tragically lost their lives in a series of destructive forest fires that started in Yunnan Province in southwest China in March 2024. The worst happened in Douge Village, Lincang City, where a fire broke out and three people died. About 3,000 residents had to be evacuated due to the fire's quick progress. Another person was reported dead in a forest fire near Wenshan in a different incident. Strong winds and dry weather made these flames worse and made combating them more difficult. Since then, local officials have gathered a lot of resources to fight the fires and stop more deaths (Lu et al., 2024). There were 221 forest fires in Guizhou Province, southwest China, between February 10 and February 21, 2024, including 11 mountain fires that claimed two lives. The combined efforts of 730 rescue teams, which included 15,000 local volunteers and 9,200 workers, put out the fires. Ten people were arrested by the authorities for unlawful fire use, which included anything from cigarette butts to tomb-sweeping customs.

Critical infrastructure was not significantly impacted by any secondary disasters, despite the devastation. A working group from the national forest fire prevention headquarters was sent to Guizhou to supervise rescue and firefighting efforts. A few contributing factors were extended warm weather and little precipitation, which created dry conditions that allowed flames to spread quickly (Kejun, 2020).

1.2.2. Causes and Impacts of Wildfires in Himalayan Region

There are three types of forest fires: (*i*) natural; (*ii*) intentional or arson; and (*iii*) unintentional or accidental. The most common causes of forest fires are both natural (such as lightning, rockslides, and volcanoes) and man-made (such as slash-and-burn farming, deforestation, controlled burning, firewood, campfires, hunting and poaching, tea growing, etc.) (You & Xu, 2022). Nearly 58% of all forest fire causes are intentional, which accounts for a high prevalence of forest fires. According to this analysis, agricultural uses are the primary cause of most intentional fires. For example, livestock owners should promote the development of new grass for their animals. In regions like Nepal and India where shifting farming is common, farmers purposefully cut down and burn trees to make room for crops (Kumar & Kumar, 2022). People's carelessness can also result in unintentional forest fires. Among these are smokers who purposefully start forest fires by tossing burning cigarette butts. This is a significant factor, particularly in coniferous woods during the arid months of the year (Mamgain et al., 2023).

Wildfires affect biodiversity, the natural environment, and people. They also contribute to global warming. According to studies on the effects of forest fires, both man-made and natural, on the environment and ecosystem, burning biomass results in high carbon emissions, biodiversity loss, emissions of trace gases, aerosol particles, and black carbon, the release of nearly 100 million tons of smoke aerosols into the atmosphere, a rise in surface albedo, and water runoff (Ahmad & Saran, 2024). Fires impact soil characteristics such as structure, porosity, and hydraulic conductivity in addition to consuming or severely charring vegetation (Prabhakaran & Srivastava, 2025).

There are significant effects on the diversity and density of forest ecosystems, especially in the highland areas where fires occur less frequently. Recent years have seen a rise in forest fire events in Nepal, mostly during the dry season from November to June. These fires have changed the composition, diversity, and regeneration of plants, which has led to decreased floral production, changed rates of regeneration, and the extinction of endemic and endangered species. Particularly in places without surface cover, bare soil is susceptible to erosion following fires. Different biological zones in Nepal, such as the Terai, Mid-hill, and Mountain areas, are affected differently by forest fires (Kumar & Kumar, 2022).

Approximately 172,040.65 hectares of forest land were damaged by forest fires in Nepal between 2001 and 2020, resulting in a loss of about 7.07 million tons of biomas (Chitale & Behera, 2019). Approximately 3.30 million tons of carbon are released each year because of forest fires, which are equal to 12.12 million tons of CO2, 7.69 million tons of

CO, and 4.39 million tons of methane gas. Forest fires also have a significant economic impact; in 2020–2021, it was estimated that thousands of homes and cow sheds were destroyed by flames that burned close to woods, resulting in a significant financial loss. Forest fires have tragically claimed 71 lives between 2007 and 2020 (You & Xu, 2022).

1.2.3. The Relationship between Climate and Wildfires in Himalayan Region

Wildfires are increasingly being caused by climate change. Climate anomalies enhance the probability of burning and make forest ecosystems more vulnerable to forest fires (Kumar & Kumar, 2022). The Himalayas are experiencing the effects of climate change; the region's ecosystem services have been negatively impacted by changing vegetation, land use, biodiversity loss, and cryosphere shrinkage (Prabhakaran & Srivastava, 2025). The frequency, size, and impact of forest fires have significantly increased in the Eastern Himalayas as a result of prolonged drought (caused by climate change), timber exploitation, and rapid land use changes

According to a recent simulation study conducted by to evaluate the impact of climate change on wildfire dangers in Bhutan, fire threats would double under a changing climatic scenario (Gurung et al., 2023). In their study on forest fires using remote sensing, (Gurung et al., 2023)verified that forests are more susceptible to fires due to longer dry winters and rising mean temperatures. Most forest fire incidents are associated with weather factors such humidity, rainfall, temperature, and drought. Forest fires occur more frequently and are larger in size when there is a greater drought, a warmer environment, and less precipitation.

1.2.4. Wildfire Analysis Using Remote Sensing and GIS

Remote sensing and GIS are essential for tracking wildfires at every stage of their life cycle, including determining the fuel conditions before the fire, describing the locations and emissions of current fires, and analyzing the consequences of the fire on vegetation, air quality, and climate after it has ended (Ambrosia et al., 1998). With an emphasis on their usage in following the dynamic spread of specific fire occurrences and obtaining data on emissions and burned area, this primer looks at the remote sensing tools currently in use in wildfire research (Pradhan et al., 2007).

Two important remote sensing techniques for tracking forest fires are active fire detection and burned area mapping, each with a distinct function (Fig. 2). Active fire detection looks for thermal anomalies, or hotspots, brought on by high-temperature combustion to identify active flames almost instantly. Available through NASA's Fire Information for Resource Management System (FIRMS), sensors like MODIS (Moderate Resolution Imaging Spectroradiometer) and VIIRS (Visible Infrared Imaging Radiometer Suite) offer frequent (multiple times per day) global fire observations, albeit at coarser spatial resolutions (375 m to 1 km). This makes them perfect for emergency response and real-time fire monitoring (Connell, 2015). However, burned area mapping uses vegetation reflectance changes and burn indices like the Normalized Burn Ratio (NBR) and differenced NBR (dNBR) to identify and quantify the amount of land impacted after the fire has gone (Hua & Shao, 2017).

This is typically accomplished by high-resolution multispectral satellites such as Sentinel-2 (10–20 m), Landsat-8/9 (30 m), and PlanetScope (<5 m). The need for cloud-free post-fire photography prevents burned area mapping from providing real-time information on fire scars, severity, and ecological damage. NASA's Fire Information for Resource Management System (FIRMS), for example, uses MODIS and VIIRS sensors to offer near real-time active fire locations around the world (Connell, 2015). These sites are commonly represented as 1 km thermal hotspots. Studies on wildfire monitoring have made extensive use of this approach to track fire activity, identify ignition sites, and examine patterns of fire spread. On the other hand, because of its precise spatial information and frequent revisit time, higher-resolution imagery, like Sentinel-2 (10 m), is very useful for mapping fire perimeters and determining burn severity. The value of Sentinel-2 and Landsat imagery in mountainous and forested areas has been shown in numerous studies (Ambrosia et al., 1998; Sowmya & Somashekar, 2010; Sunar & Özkan, 2001).

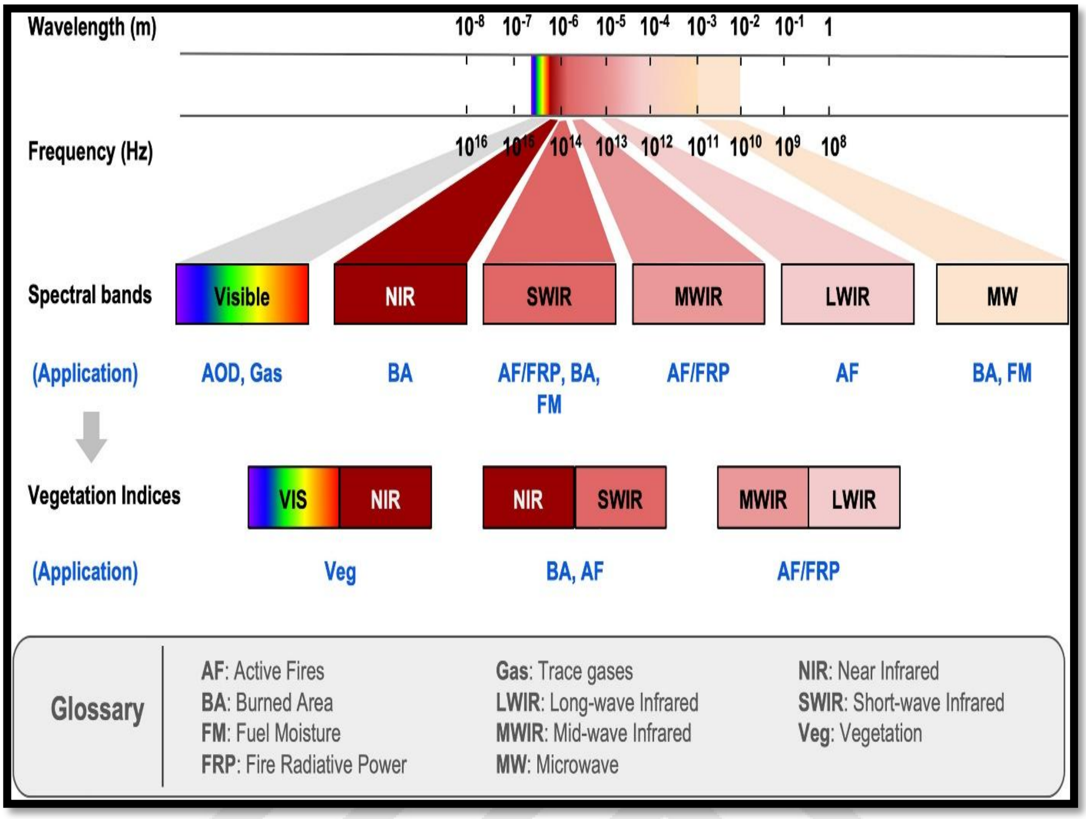

Figure 2. The use of remote sensing in wavelength-dependent ways to map burned areas, measure fire emissions, and monitor ongoing fires

Accurate burn-area estimation, both quantitatively and qualitatively, is essential for assessing how fire affects forests. Google Earth Engine uses the medium resolution optical-satellite imagery of Landsat-8 and Sentinel-2, which spans the years 2016 to 2019, to identify forest fire areas(L. Yang et al., 2022). In Uttarakhand, India's western Himalaya, the pre-monsoon season is the most crucial time of year for forest fires(R. D. Singh et al., 2024). To extract the burn area, they used techniques like visual interpretation, the difference between Normalized Difference Vegetation Index (NDVI), and the differenced Normalized Burn Ratio (dNBR). The findings showed that, with a coefficient of determination (R^2) higher than 0.96, the three monitoring techniques were quite consistent. Furthermore, the majority (58.05%) of the impacted regions were caused by moderate-severity fires, according to an analysis of fire severity using a threshold method based on dNBR-extracted burned areas. Additionally, the study discovered that topographic characteristics such as northwestern aspects, steep slopes, and high elevation significantly impacted the intensity of fires (Piepho, 2019).

1.2.5. Wildfire Dynamics and Fire Behavior

Understanding wildfire dynamics and creating effective mitigation plans require modeling fire behavior, including rate of spread, direction, severity, and duration. Among the most popular foundational models is Rothermel's fire spread model, which uses wind speed, slope, and fuel moisture to mathematically characterize fire propagation in homogenous fuels (Finney et al., 2021). Simulation-based methods, such FlamMap and FARSITE, which employ meteorological and spatial inputs to model fire growth, have been included into more contemporary methodologies (Speer & Goodrick, 2022). The rate of spread and flame length are the two most important and useful estimates for scientists, first responders, and fire control agencies involved in decision-making, even though many environmental factors can concurrently affect a wildfire's behavior. It is commonly acknowledged that the most important factors affecting the behavior of wildland fires are; fuels, topography and weather (Silva et al., 2022).

However, simulating fire behavior is extremely difficult in areas like the Himalayas that have complicated topography and little ground data. Because of challenging terrain, restricted field access, and a variety of vegetation types, high-resolution fuel data which are essential for precise simulations are sometimes in little supply or non-existent (H.-H. Wang et al., 2025).

2. MATERIALS AND METHODS

2.1. Study Areas

The Himalayan Mountain range, which spans more than 2,500 km over Pakistan, India, Nepal, Bhutan, and Tibet (China), is one of the youngest and most dynamic mountain systems on Earth. The Himalaya is separated into four horizontal divisions: the western Himalaya, which includes the Himalayas of Jammu and Kashmir, Himachal, and Uttarakhand; the central Himalaya, which includes the Nepal Himalaya; the eastern Himalaya, which includes the Sikkim and Arunachal Himalayas; and the eastern extension, which includes Nagaland, Manipur, Mizoram, Tripura, Meghalaya, and the hills of West Bengal and Assam. Scholars from various disciplines who work in the Himalaya have studied specific aspects or regions (R. B. Singh, 2016).

From tropical forests at lower elevations to glaciers at the highest point, the climate and vegetation change significantly with terrain height. In just a few kilometers, the terrain changes from 300 meters (tropical lowlands) to over 8,000 meters (high mountains), resulting in the emergence of a wide variety of ecozones. Because of this, the Eastern Himalayan region has an extremely rich ecosystem with a high degree of endemism and a very diversified biodiversity (Pathak et al., 2023). Wet evergreen, semi-evergreen, moist deciduous, coniferous, mixed, temperate, and shrubland forests are among the major reserves of tropical and sub-tropical forests that may still be found in this area (Joshi et al., 2024).

2.2. Climate of the Himalayan Region

The climate of the Himalayas varies greatly depending on the geography, altitude, and local weather patterns. The dry season, which usually lasts from late autumn to spring (November to May), is one of the most significant climatic factors affecting the occurrence of wildfires. Particularly during the pre-monsoon months (March to May), there is little precipitation and rising temperatures at this time, which makes it perfect for fires to start and spread (S. Singh et al., 2016).

The summer monsoon (June–September) follows this dry season, bringing with it a lot of rain, more moisture for the vegetation, and a significant reduction in fire activity. The length and severity of the fire season, however, differ throughout the Himalayan range. In addition to delaying the fire season, the Western Himalayas which include parts of Pakistan, Uttarakhand, and Himachal Pradesh frequently receive winter precipitation or snowfall (Chauhan et al., 2023). In contrast, the fire window is sometimes shortened in the Eastern Himalayas, including Bhutan and Northeast India, due to early and heavy monsoon rains (Bhattarai et al., 2022). Although temperatures typically drop with height, foothill areas such as the Terai and lower Shiwalik Hills are particularly vulnerable to fire outbreaks because they can get extremely hot and dry during the pre-monsoon season (Bhattarai et al., 2022).

2.3. Socio-Environmental Context in the Himalayan Region

Millions of people reside in the Himalayan region, where their livelihoods are mostly dependent on natural resources. In several locations, the hill and foothill regions are heavily populated, with local populations reliant on small-scale farming, forestry, and cattle grazing. Because of this, there is a significant contact between human activity and forested areas, which raises the possibility of forest fires caused by humans (Bhattarai et al., 2022). People in hill and mountain communities frequently encounter fire-prone areas because they rely so significantly on forest resources for fuelwood, fodder, and non-timber forest products. In regions of Nepal, Northeast India, and Bhutan, traditional land-use activities like seasonal grassland burning for pasture renewal and slash-and-burn agriculture (jhum farming) are frequently carried out without proper fire control measures (Rajan Kotru et al., 2015).

Climate change is making rural populations in the Himalayas more susceptible by prolonging fire seasons and drying fuels. In addition, a lot of these areas have poor fire governance, with little public knowledge, fire detection, and suppression capabilities. Although community forestry programs have been implemented in locations like Bhutan and northern India, proactive fire management is hampered by a lack of institutional support and enforcement (Vilà-Vilardell et al., 2020; Zinck & Grimm, 2009).

2.4. Environmental Conditions of Study Sites

Eight wildfire incidents were chosen for analysis in this study, and they represent a range of topography and ecological zones in the Himalayan region, including differences in vegetation types, land use patterns, and conservation designations. The mid-hill and lower montane zones, which are dominated by mixed broadleaf forests, Blue pine (*Pinus wallichiana*), and Chir pine (*Pinus roxburghii*). Because of their seasonal dryness, needle litter, and resinous vegetation, these forest types are especially prone to fire (Bhattarai et al., 2022; Vilà-Vilardell et al., 2020).

Particularly in Nepal and northern India, several of the burned sites are inside or close to community forests, where local forest user organizations oversee the management of forest resources. For instance, a patchwork of community forests with high pine cover that had accumulated a significant amount of leaf litter because of extended dry conditions, and a lack of forest floor clearing was impacted by the Makwanpur Hills Fire (2021). Like this, the Debsi Fire (2023) in Bhutan happened in a degraded mixed forest area on sloping terrain where fuel accumulation and prior fires had made the area dangerous.

Other fires, like the Margalla Hills Fire (Islamabad, 2024), happened in protected locations, including national parks, where access and rough terrain frequently restrict firefighting efforts (Tariq et al., 2020). Conifer-dominated upper montane forests in steep Himalayan valleys that had seen below-normal winter precipitation were impacted by the Kyirong Fires and the Juwagwar Forest Fire, indicating a connection between seasonal drought and heightened fire vulnerability (Suyal et al., 2022).

Blue pine woods on south-facing slopes, where drying is accelerated by wind and sunlight, were destroyed by the Trishuli Fire in Nepal. Fire control is a top priority because many of these woods are located close to growing wildland-urban interfaces, which pose a risk to infrastructure and habitations.

2.5. Selected Wildfires in the Himalayan Region

In this study, eight typical wildfire incidents that have taken place in various Himalayan regions between 2016 and 2025 are examined. These incidents were chosen because of factors such the availability of high-quality satellite imagery, geographic distribution, fire intensity, and data availability. Instead of regularly assessing the entire Himalayas, the study deliberately looks at these instances to document temporal and regional diversity in perimeter expansion, fire behavior, and affecting climate conditions. The chosen events encompass a variety of ecozones and elevations in Pakistan, India, Nepal, Bhutan, and Tibet (China). The name, location, time frame, and projected total area burned are recorded for every fire incident. While some of these fires happened during recognized dry spells, others stood out for their quick spread, proximity to populated areas, or ecological harm (Table 1).

Table 1. The Selected Himalayan wildfire incidents from 2016 to 2025 along with their locations and time frames.

No	Fire Name	Location/Region	Dates	Total Area burned (ha)
1	Galiyat Forest Fire	Pakistan (KPK)	31-12-2020 to 01-01-2021	191
2	Debsi fire	Bhutan (Thimphu)	22-02-2023 to 23-02-2023	421
3	Lachung forest fire	Sikkim, India	26 to 28-01-2023	108
4	Uttarakhand forest fires	Uttarakhand, India	24 to 25-05-2020	284
5	Trishigang Fire	Bhutan (Thimphu)	18 to 21-02-2022	1040
6	Kyirong, Tibet forest fire	Sichuan Province, China	23-01-2025 to 08-02-2025	1504
7	Juwagwar forest fire	India	05-01-2024 to 07-01-2024	508
8	Manang Fire	Kathmandu, Nepal	07-01 to 12-01 & 26-01 to 29-01-2021	1417

Insights into the ways that ecological diversity, climate variability, and human influences interact to produce fire regimes throughout this delicate mountain system were supplied by the collective sites, which together offered a representative cross-section of wildfire dynamics in the Himalayas.

2.6. Wildfire Perimeter Mapping Methodology

To accomplish the first objective, which was to map the perimeters of wildfires throughout the Himalayan region from 2016 to 2025, this study used data from active fire detection with satellite-based remote sensing. NASA's Fire Information for Resource Management System (FIRMS), which uses thermal anomaly detections from MODIS (Moderate Resolution Imaging Spectroradiometer) and VIIRS (Visible Infrared Imaging Radiometer Suite) sensors at a spatial resolution of about 1 km to provide worldwide fire alerts, was used to identify ten major wildfire events (Falkowski et al., 2024). Fire intensity, location, size, and the availability of cloud-free Sentinel-2 footage close to the incident were taken into consideration while choosing events. Copernicus Data Space Ecosystem imagery was used to acquire Sentinel-2 Level-2A images. The pre-fire and post-fire Normalized Burn Ratios (Pre NBR and Post NBR) were computed using the 20 m resolution bands 8A and 12. After that, the differenced Normalized Burn Ratio (dNBR) was calculated to determine the extent of the burn. To identify burn scars, pre-fire and post-fire images were visually compared.

These images were found to have increased reflectance in the shortwave infrared bands and a darkened spectral response in the visible and near-infrared bands, which is consistent with post-fire char and ash signatures (Tiengo et al., 2025). In short, utilizing pre- and post-fire NBR, burned regions were mapped using a conventional remote sensing methodology. Regarding every fire:

1. Sentinel-2 Band 8A (NIR) and Band 12 (SWIR) were used in QGIS to calculate the NBR before and after the fire.
2. After then, dNBR was computed by deducting post-fire NBR from pre-fire NBR.

3. The reclassification of dNBR adhered to the conventional USGS fire severity levels (unburned, low, moderate, and high).
4. To ensure precise perimeter delineation, the dNBR raster was polygonized to produce vector borders of burned regions.
5. VIIRS hotspot data were used to rebuild the daily perimeters. The final fire scar was divided into daily polygons using QGIS's "Split Feature" tool, which showed how the fire front grew over time.
6. The QGIS field calculator was used to calculate the burned area, and the polygon area was converted to hectares using the method $area/10000.

Through this process, a time series of daily fire spread polygons, and the total burned area for each fire were generated.

Burned area was calculated with Sentinel-2 L2A satellite imagery using Band 8A (near-infrared) and Band 12 (shortwave infrared). The images before and after fires were taken and Normalized Burn Ratios were calculated as:

a) Pre-NBR (before the fire)

b) Post-NBR (after the fire)

To calculate the Differenced Normalized Burn Ratio (dNBR), Pre-NBR is subtracted from Post-NBR that reflect how much of vegetation was burned during the fire. In QGIS 3.34, reclassification tool is used to classify burned and unburned areas. Burned area polygons for each fire and each day were digitized from rasters, and total area was calculated with QGIS Field Calculator function. Polygons area were converted into hectares using the formula:

$$\text{Burned Area in hectare} = \frac{Area\ (m2)}{10000} \quad (1)$$

Daily burnt area for each fire was calculated in this way. Daily burnt area were then compared to WFA pocket results to validate the model predictive performance across each wildfire event.

2.7. Rate of Fire Spread (ROS) Calculation

Using the distance between subsequent fire perimeters, the ROS was calculated (Abouali & Viegas, 2019). Regarding every day:

1. A measurement was made of the centroid-to-centroid distance between successive polygons.
2. ROS was computed using the formula ROS = ΔDistance / ΔTime, where time was expressed in hours and distance in kilometers, yielding ROS in kilometers per hour.
3. A uniform dataset for all eight fires was produced by entering ROS values into the attribute table of each fire's perimeter shapefile. To assess the accuracy of the model, these data were subsequently averaged and contrasted with the predictions of the simulator.

2.8. Fire Behavior Simulation

The WFA Pocket Fire Behavior Simulator was used to study wildfire dynamics. This tool estimates fire spread by combining fuel, topography, and meteorological parameters. Temperature, relative humidity, dead/live moisture conditions, slope, aspect, wind direction and speed, and fuel type were all necessary inputs. The simulator was used to run simulations for every fire, considering the fuel assignments and observed weather conditions. Burned area (ha) and projected ROS (km/h) were among the outputs. Despite being oversimplified, this tool offered a foundation for comparing how fire behaved in various scenarios.

Sentinel-2 L2A imagery (dNBR) and VIIRS active fire detections were used to rebuild the observed daily perimeters and burned areas; the inter-day perimeter advance was used to determine the observed ROS. Fuel maps (ESA World Cover mapped to Anderson fuel models), DEM-derived terrain (slope, aspect), and ERA5 reanalysis (wind, temperature, and dew point) were used as simulator inputs. Pooled Bias (Predicted − Observed) and adjusted coefficient of determination (Adjusted R^2) for each of the 40 fire days are used to summarize model performance, in accordance with the validation methodology employed in the reference literature.

2.9. Statistical Analysis and Validation for Model

The observed ROS and burnt area were used to assess the WFA Pocket Simulator's performance. The formula for calculating bias was Bias and R^2 and Adjusted R^2 metrics were used to evaluate model fit. Microsoft Excel programme was used to create scatterplots of predicted versus observed values, and Python was used to calculate validation measures. Model validation was based on Adjusted R^2 and bias values from the combined dataset of all eight fires.

NASA FIRMS was used to identify fire occurrences, and Sentinel-2 imagery was processed to map burned areas and perimeters and calculate NBR/dNBR. To compute ROS and environmental drivers, topography factors, fuel data, and meteorological variables (ERA5) were then obtained. Lastly, WFA Pocket simulations were run using these inputs to forecast fire behavior (Fig 3).

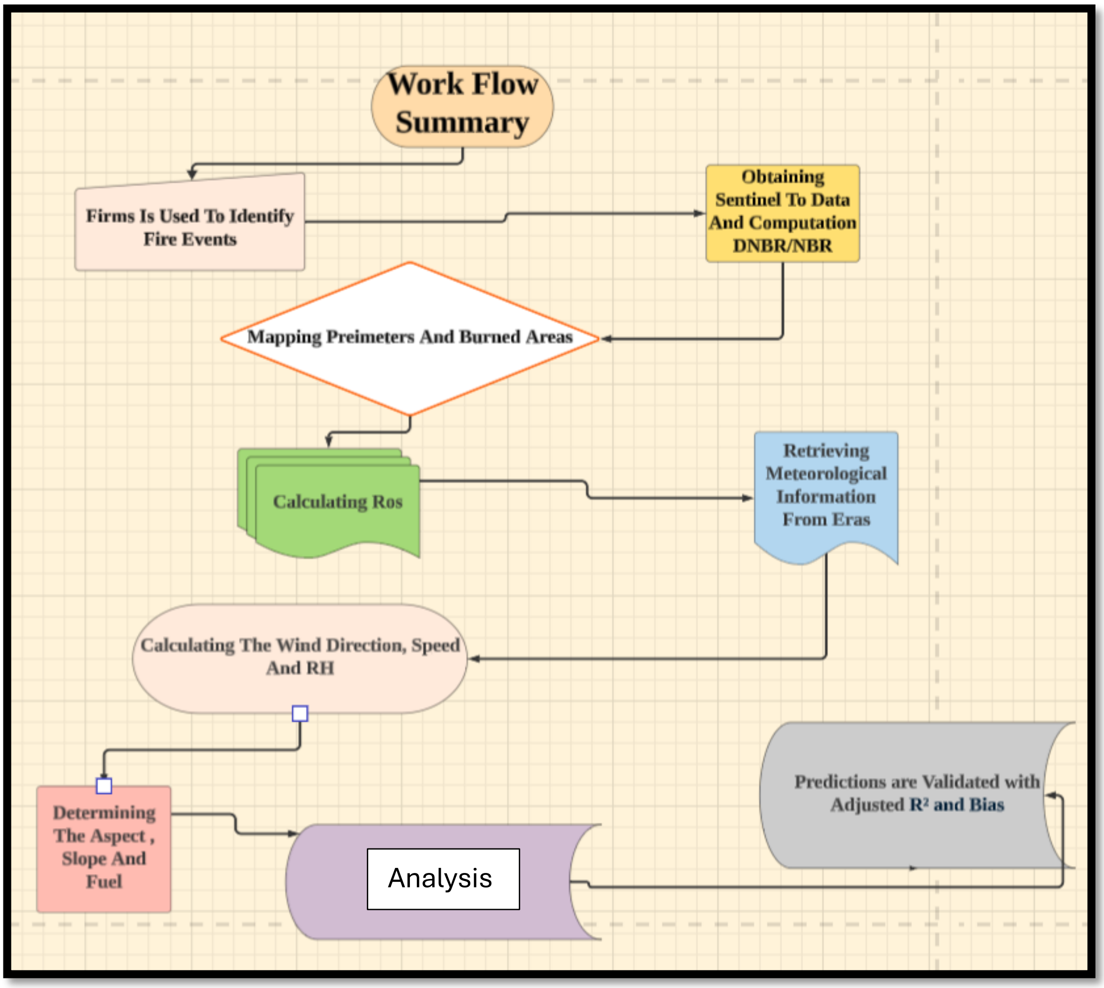

Figure 3. The Workflow for validating and simulating of selected wildfires

Both statistical and graphical studies were performed to assess model performance and analyze wildfire dynamics. Daily comparisons of actual and simulated burned areas, temporal patterns in ROS, and changes in fireline intensity over the course of each fire occurrence were among the key graphs. QGIS (version 3.34.11) was used for geospatial analysis and mapping, and Python modules including xarray, rasterio, geopandas, and matplotlib were used for data preparation, spatial statistics, and personalized visualizations. Furthermore, validation graphs comparing observed and simulated results were created using Microsoft Excel, offering a transparent evaluation of the predicted accuracy of the model. This study's statistical analysis and validation are based on the two equations mentioned below (Ruiz Gonzalez et al., 2009; S. Singh, 2018).

Formula for Bias: $\frac{1}{n}\sum_{i=0}^{n}(yi - y\hat{}i)$ (2)

Adjusted coffecient of determination R^2adj= 1-$\frac{\sum_{i=1}^{n}\frac{(yi-y\,i^{\wedge})2}{n-p}}{\sum_{i=1}^{n}\frac{(yi-y)2}{n-1}}$ (3)

3. RESULTS AND DISCUSSION

3.1. Uttarakhand Fire Event, Observed Dynamics and Simulation Performance

The May 2020 fire in Uttarakhand provides a touchstone for comprehending model observation divergence and provides a thorough example of pre-monsoon fire behavior in a high, patchy Himalayan region (Fig 4). The occurrence took place in the foothills of Garhwal, where southern aspects and elevations combine to create late-spring fuel beds that dry quickly.

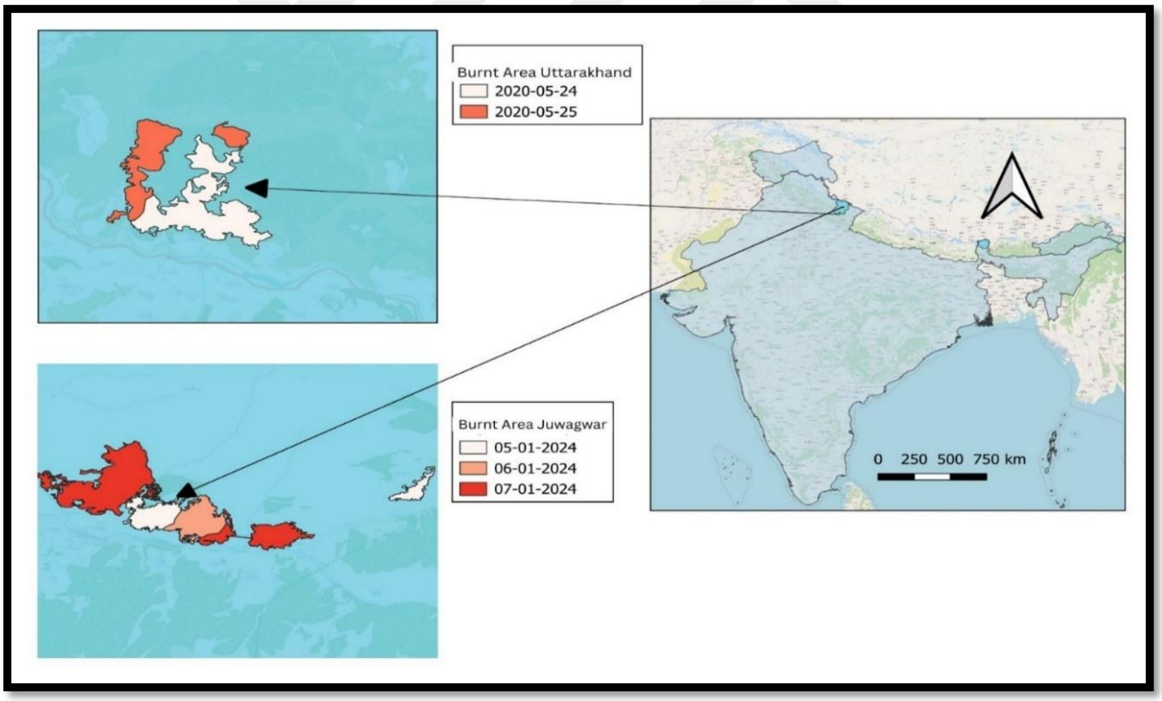

Figure 4. The daily progression of Uttarakhand fire in India

Relative humidity frequently dropped below 40% during the hottest parts of the day, while the local weather throughout the event was marked by daytime temperatures above 25 °C and constant valley winds of 15–20 km/h. According to the ESA WorldCover vegetation map, there were sporadic chir pine trees and shrub patches amidst a predominant grass matrix. The simulator was parameterized using fuel classes that approximated Anderson's GR2 model, and these conditions correspond to a mixed grass/shrub fuel environment.

The daily segmentation showed a fire that advanced in pulses, with more fast runs connected to abrupt increases in wind speed between days of modest advance. Slope and aspect had significant spatial control on the spread; the most active fire fronts were found on south and southwest-facing slopes because of higher insolation and reduced fuel moisture. Small rock outcrops, damp hollows, or agricultural clearings were examples of fuel discontinuities that commonly interrupted continuous spread, resulting in patchy charred mosaics as opposed to uniform perimeter expansion. The model generated consistently greater ROS and, as a result, bigger daily burned areas when it was duplicated in WFA Pocket using inputs from ERA5 and the previously specified terrain/fuel assignment. On average, simulated ROS values were 30–50% higher than those recorded during the incident. The model produced smoother, more continuous perimeter growth in response to sustained wind forcings and upslope propagation.

The fire behavior stands in contrast to the pattern that was seen, which showed that stalls and local extinctions were typically caused by heterogeneity and micro-scale weather fluctuations. On some days, the simulated increase almost quadrupled the actual increment, resulting in a significantly greater cumulative area by the end of the event. Simulator burned area aggregates showed a consistent positive offset in comparison to observations. Interpreting the discrepancy reveals several interrelated factors.

First, although ERA5-based inputs offer consistent synoptic and regional forcing, they could miss local inversions and valley-scale wind accelerations, which have a big impact on fire dynamics in mountainous areas. Second, even though Himalayan grasslands frequently exist as a mosaic with variable fuel continuity, the mapping from coarse land-cover classifications to Anderson fuel models assumes uniform fuel behavior inside model grid cells. Third, the internal propagation mechanics of WFA Pocket do not incorporate fine-scale process representations for transient fire breaks, instead emphasizing continuous spread along favorable sides and slopes. Together, these variables result in a consistent overestimation of ROS and area for Uttarakhand (Fig 5 & 6).

The overall temporal trend (faster spread on windier days) was nevertheless captured by the model, suggesting that the physics base is essentially sound but needs higher-resolution inputs or local calibration to more closely match observed magnitudes. A common aspect throughout all the research events is highlighted by the Uttarakhand case: general trend reproduction but magnitude disagreement. These findings suggest that sub-daily, locally downscaled meteorological inputs must be integrated to capture transient gusts and valley circulations that drive brief high-ROS episodes, or regional calibration of fuel parameters and moisture response curves is required for operational application in comparable Himalayan contexts.

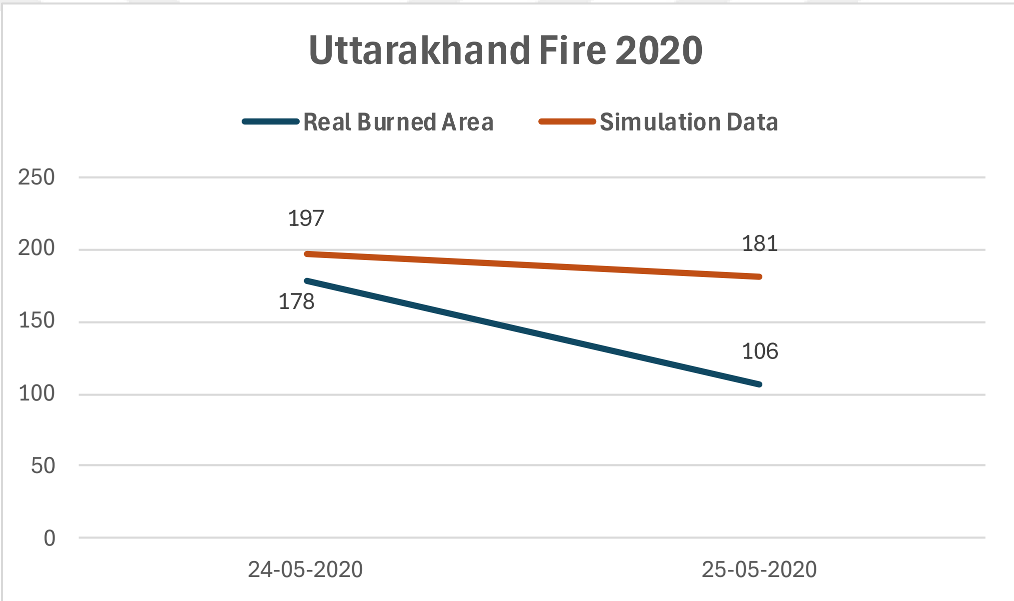

Figure 5. The observed and predicted burned area in Uttarakhand Fire.

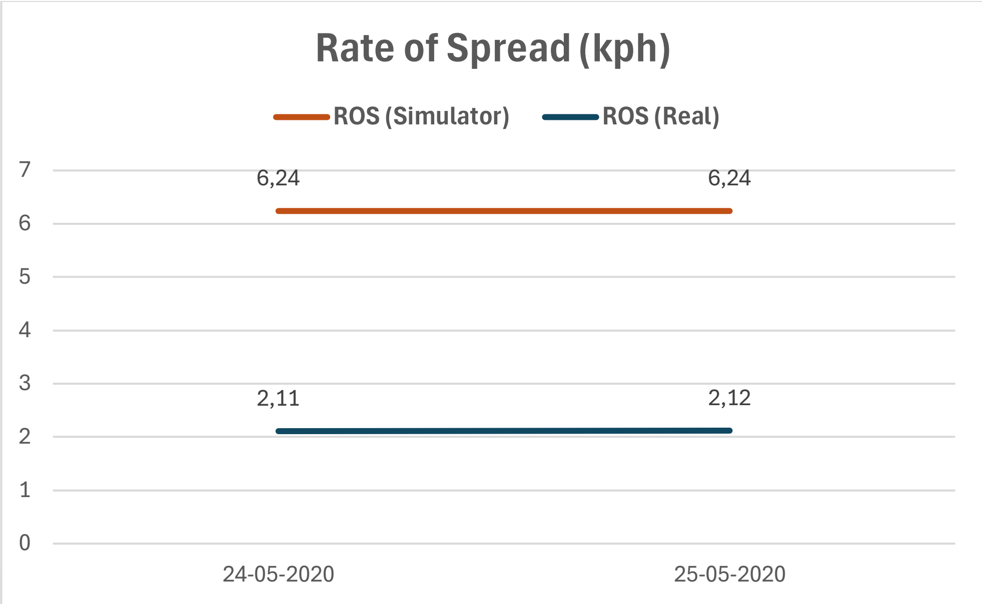

Figure 6. The observed and predicted rate of rate spread values in Uttarakhand Fire

3.2. Debsi Fire Event, Observed Dynamics and Simulation Performance

The Debsi fire in Bhutan (February 2023) takes place in an environment with lower temperatures and unusually high relative humidity, it provides a useful comparison to the Uttarakhand incident (Fig 7). With maximum daytime temperatures of about 10 °C and relative humidity levels ranging from 50% to saturation in the early morning, the occurrence occurred outside of the typical pre-monsoon window. The impacted region was topographically characterized by moderate slopes (25–35%) with a preponderance of southeast aspects. Grass-dominated cover (GR2) with scattered shrub patches was shown via fuel mapping. The high humidity level had a significant impact on the observed fire behavior.

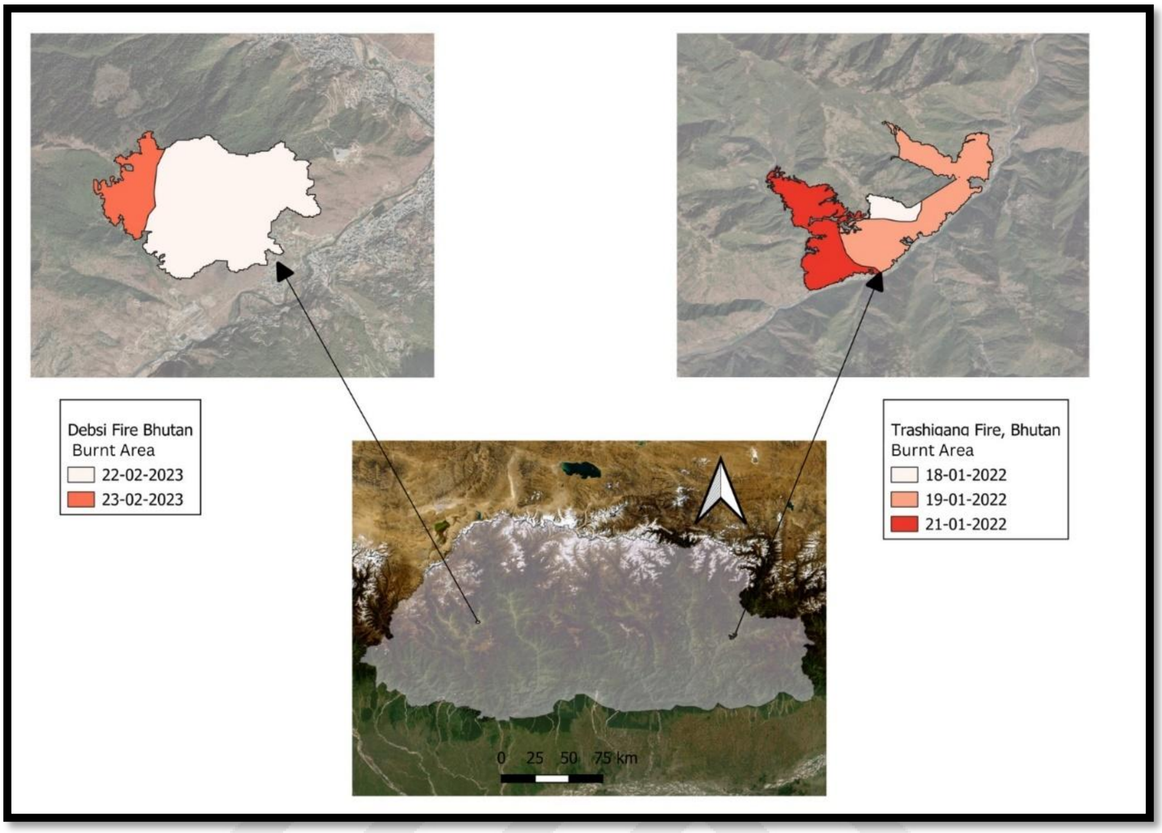

Figure 7. The daily progression of Debsi Fire in Bhutan

Compared to the first day, Sentinel-2 dNBR polygons exhibit a noticeable decrease in active perimeter growth. Lower active fire counts on day two were corroborated by VIIRS detections, indicating either suppression or fuel dampening. WFA Pocket runs using the designated GR2 fuel class and ERA5 daily means replicated the slowdown's indication but not its amount. A positive bias resulted from the fact that, although the absolute values of projected ROS were greater than observed, the simulated ROS dropped from day one to day two. Day one simulations produced less burned area than was seen in a single run, but day two simulations still created more area than was measured, suggesting that bias behavior varied from day to day (Fig 8).

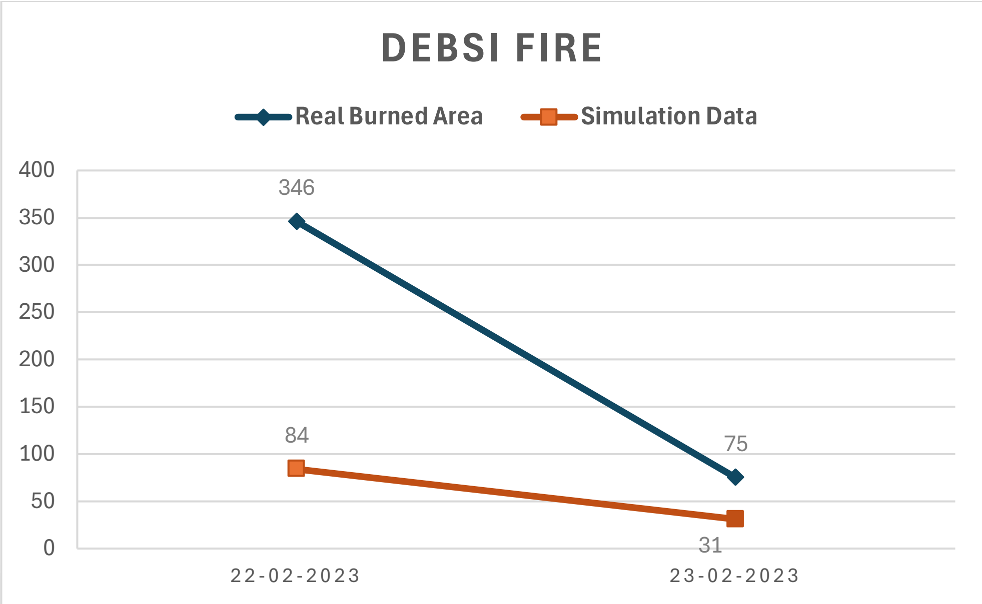

Figure 8. The observed and predicted burned area in Debsi Fire.

This erratic skew between days indicates that the model is sensitive to initial conditions and emphasizes how even minor variations in wind speed or fuel moisture input can have a significant impact on integrated area results when fires are close to the threshold for continuous spread. Debsi shows that in high-humidity Himalayan environments, the simulator needs to employ either a more sensitive mapping of humidity to fuel flammability or sub-daily near-surface humidity products to record nocturnal and early-morning saturation events that stop the spread of fire (Fig 9).

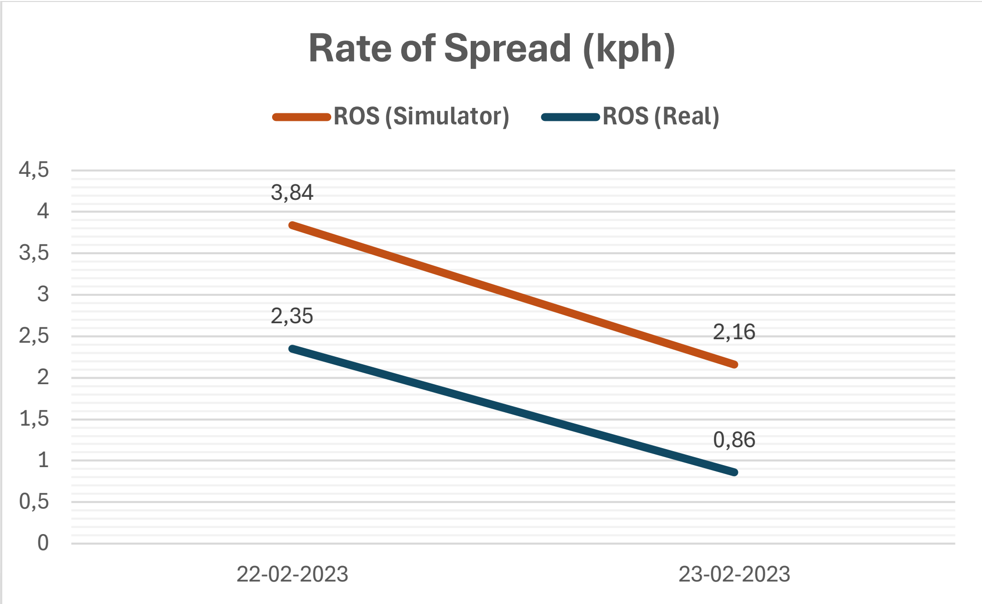

Figure 9. The observed and predicted rate of rate spread values in Debsi Fire

3.3. Manang Fire Event, Observed Dynamics and Simulation Performance

Two remote ignition clusters that happened under different synoptic conditions are combined in the Manang fires in Nepal in January 2021 to create a complicated, multi-phase scenario. A substantial propagation phase in late January was followed by an early phase of modest, patchy growth, according to the reconstruction of recorded perimeters (Fig. 10).

ROS observed during the Manang episodes varied from sub-kilometer daily advances on days of quiescence during times of increased canyon winds. The local topography played a significant role in determining the pattern of spread: fires moved quickly along lee slopes and valley corridors where wind was directed, but they halted when they came across wetter areas or sudden topographical breaks. The perimeters produced from the dNBR showed a convoluted scorched mosaic instead of a straightforward, continuous front.

The time of the greater propagation phase was matched by WFA Pocket simulations parameterized for Manang, although ROS magnitudes were frequently exceeded. Often, projected daily ROS and simulated area growth were 25–60% higher than observed levels. While observed continuity was fractured, continuous fuel stretches were treated as available for uniform dispersion by the simulator's perimeter integration. As a result, the model's supposition of a uniform fuel response within a cell generated more extensive effective spread channels than those that were found on the ground.

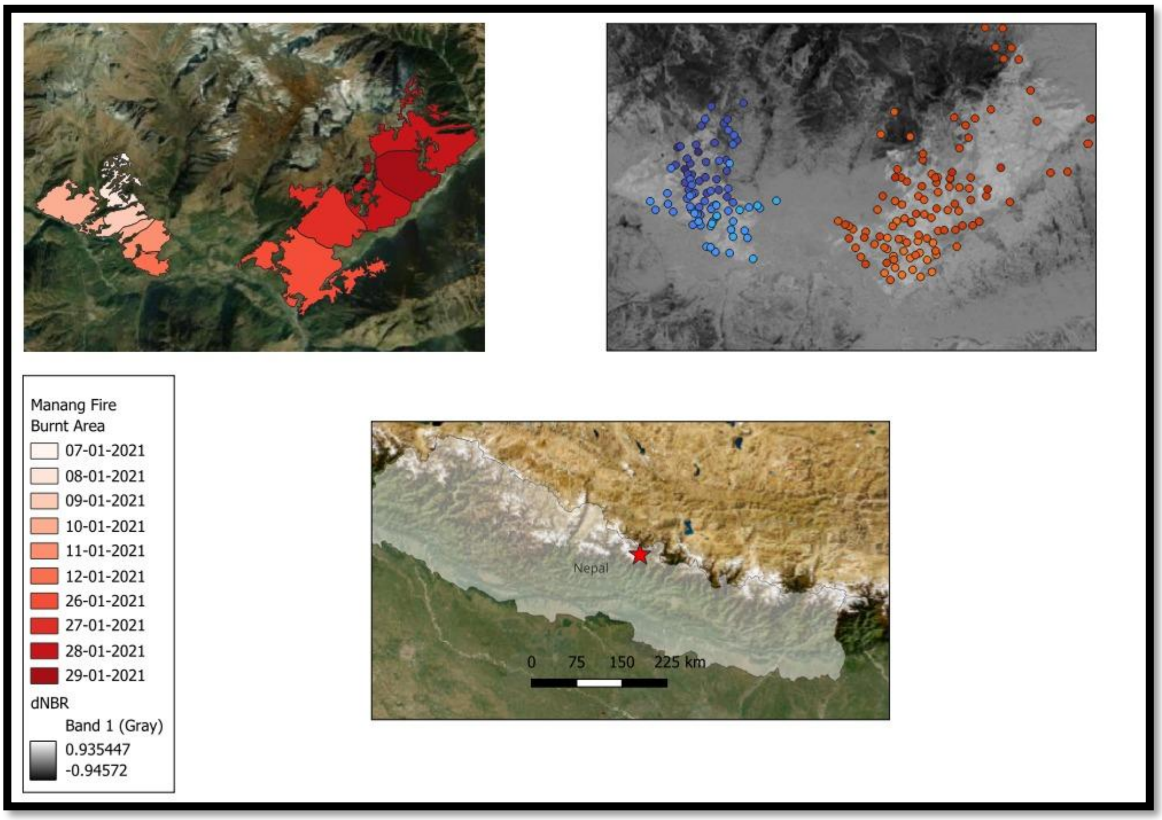

Figure 10. The daily progression of Manang fires in Nepal.

The Manang instance demonstrates how sub-daily meteorological and fuel discontinuity interact. A model without sub-daily forcing will average these effects in valleys where short gust events lead to rapid expansion, which frequently lowers peak ROS but strangely increases integrated daily spread when wind bursts coincide with favorable aspects. Furthermore, the continuous spread assumption of the simulator may result in sudden jumps in the predicted burned area that do not correspond with the gradual coalescence seen in satellite-derived perimeters when an event crosses a threshold where fuel connectivity changes (for instance, when separate patches coalesce).

From a pragmatic standpoint, Manang emphasizes why model evaluation based on daily perimeters frequently yields poor adjusted R^2 in diverse terrains: the model frequently determines "when" growth occurs but not "how much" growth will be caused by the combination of patchy fuels and brief wind bursts. Higher-resolution fuel mapping, explicit modeling of fuel discontinuities, or the application of finer temporal meteorological drivers that capture gust timing are all necessary for improving predictions in these kinds of situations (Fig 11, 12, 13 & 14).

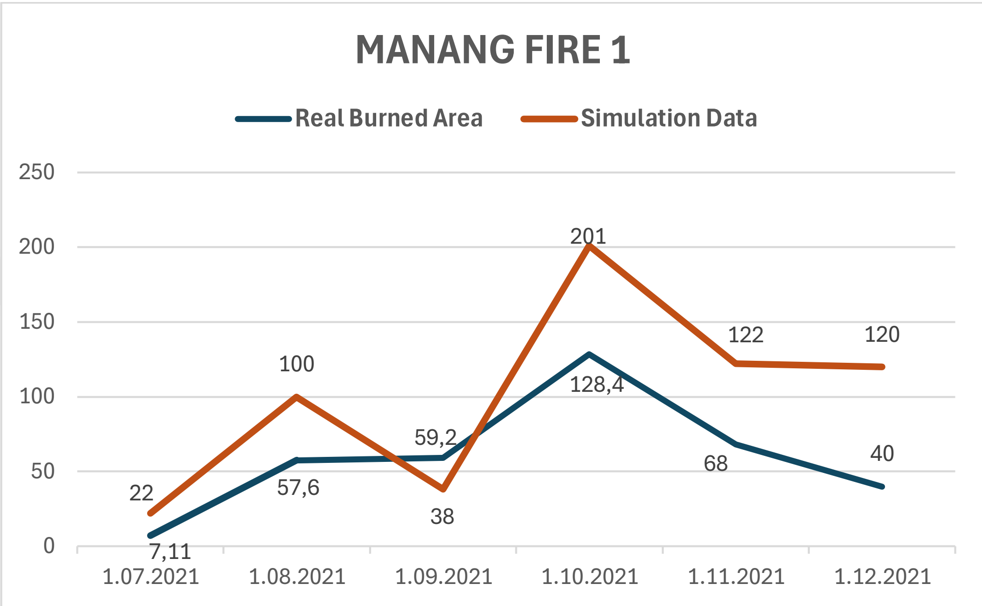

Figure 11. The observed and predicted burned area in Manang Fire 1.

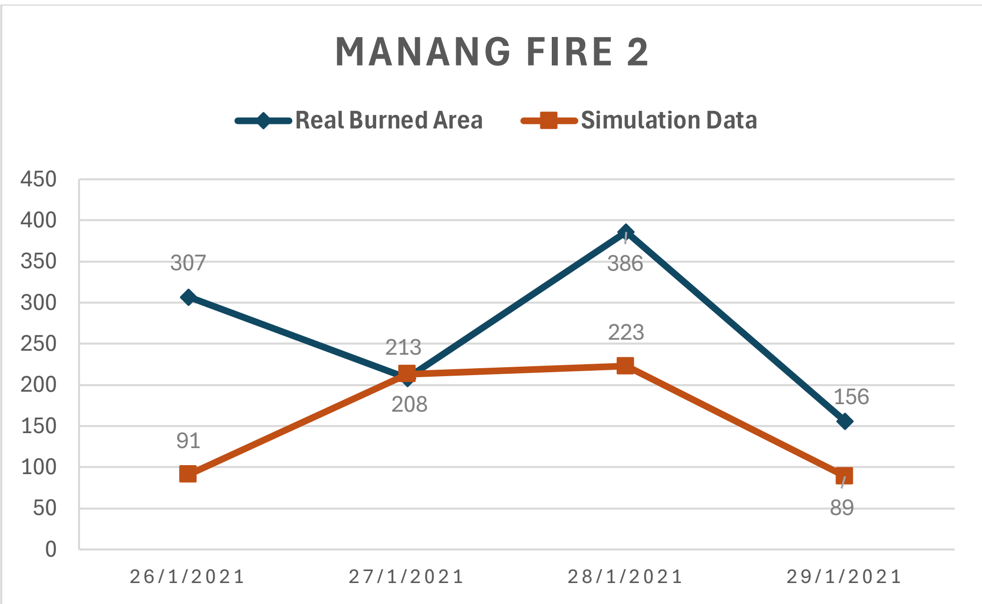

Figure 12. The observed and predicted burned area in Manang Fire 2

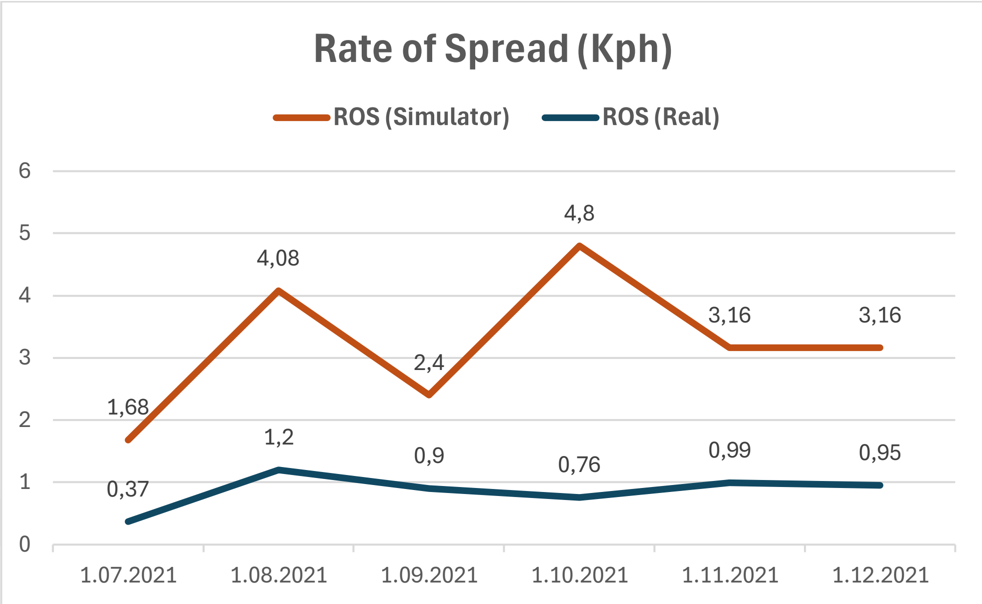

Figure 13. The observed and predicted rate of spread in Manang Fire 1

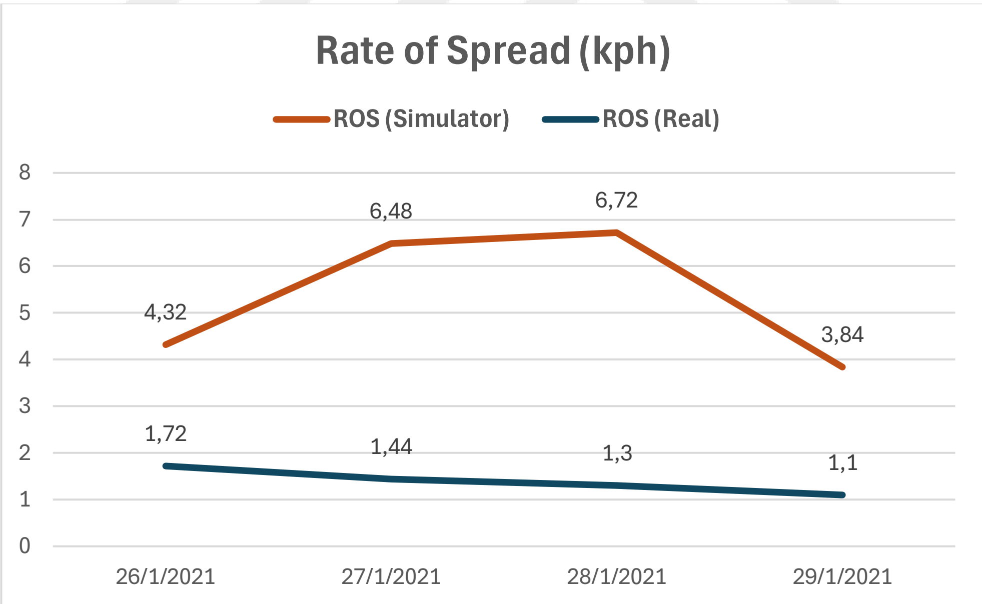

Figure 14. The observed and predicted rate of spread in Manang Fire 2

3.4. Kyirong Fire Event, Observed Dynamics and Simulation Performance

The longest-duration event in this study, the Kyirong fire in the Tibet Autonomous Region (January–February 2025), sheds light on the dynamics of prolonged fires under enduring valley winds. The perimeters that have been observed exhibit lengthy, ribbon-like expansions that run parallel to the valley floor. These expansions are punctuated by brief stalling events during which the winds change or decrease. ROS measurements had episodic peaks and ranged from 1 to 3 km/day on average. In accordance with wind-dominated propagation in limited valley geometry, the overall development produced elongated lobes rather than rounded perimeter growth. Over the course of the multi-week incident, the dNBR-derived burned area showed a significant cumulative area (Fig 15).

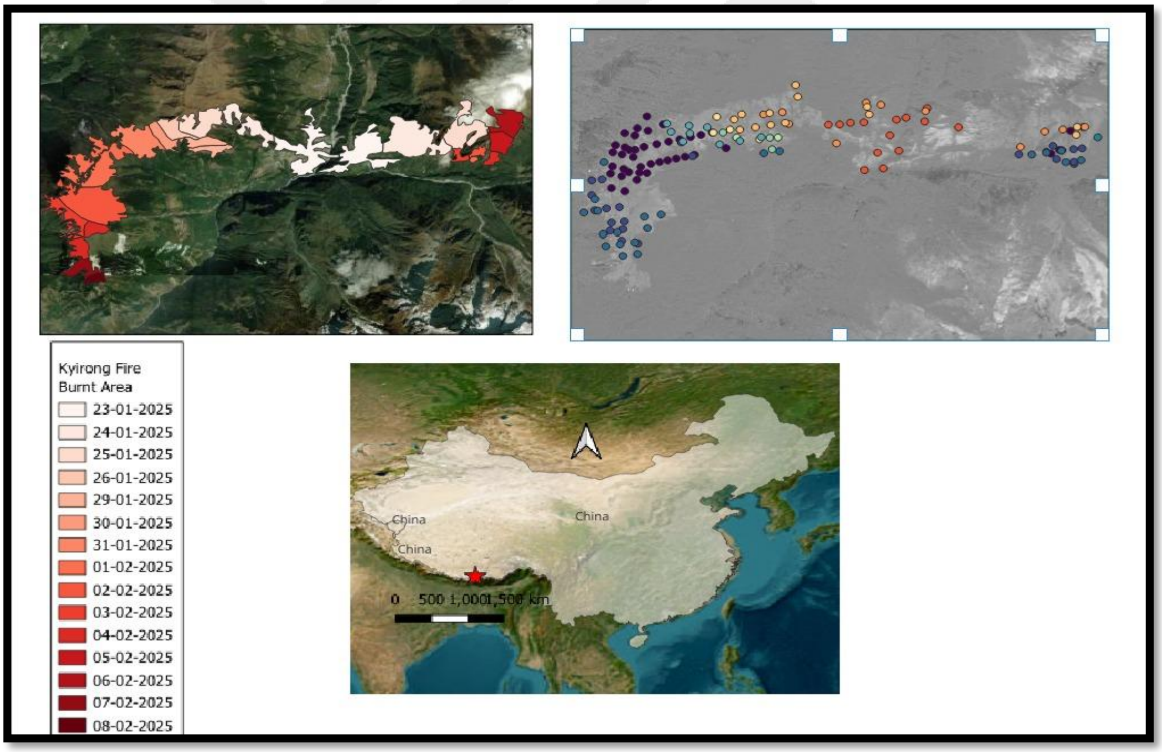

Figure 15. The daily progression of Kyirong fire in Tibet, China

The model overstated the daily advance rates while accurately capturing the directional trend of valley-parallel spread when it was replicated in WFA Pocket. The model tended to predict smoother, more continuous expansion than the observed pattern of pulses and pauses, and the simulated ROS values were typically 30–60% greater than the observed values, depending on the day. The continued positive bias in ROS and area for Kyirong again highlights the combined effects of fuel-mapping limitations and meteorological averaging: the mapping of heterogeneous grass/shrub mosaics to a single fuel class smooths effective resistance to spread, while ERA5 daily means do not represent peak gusts or sub-daily variability that may cause short bursts of rapid spread (Fig 16 & 17).

Due to Kyirong's prolonged duration, cumulative errors were able to worsen as the event went on, the simulated and observed cumulative burned area diverged increasingly due to the constant overprediction of daily ROS. The scenario demonstrates how models calibrated with broad fuel assumptions and driven by daily mean weather may have special difficulties with long-duration, wind-driven events.

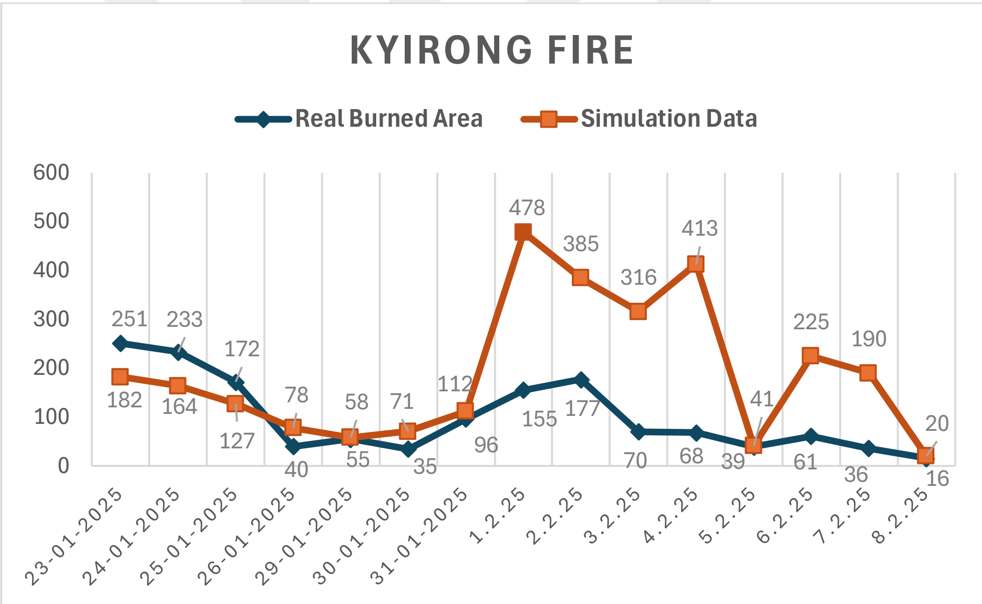

Figure 16. The observed and predicted burned area in Kyirong Fire.

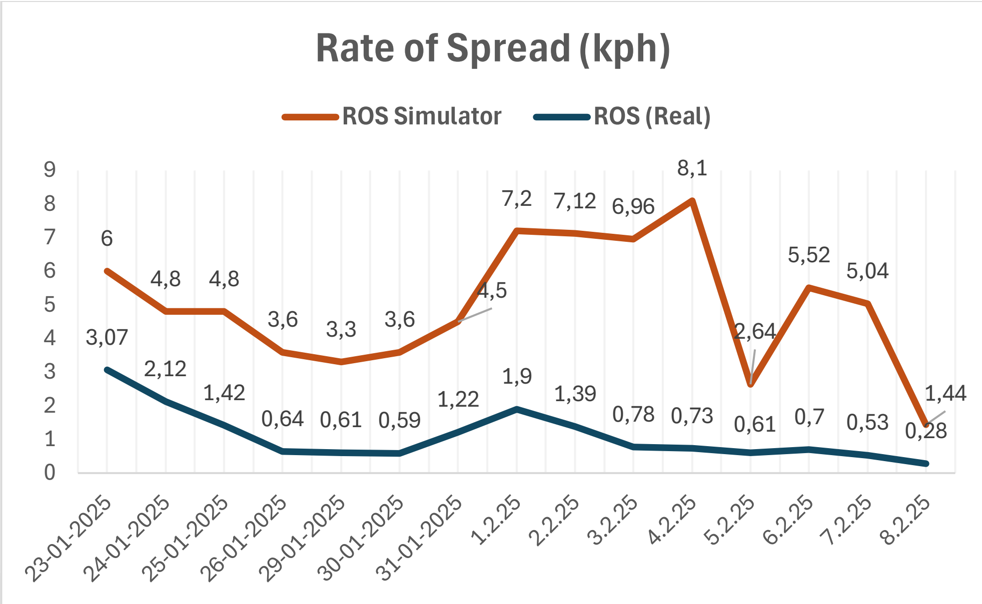

Figure 17**.** The observed and predicted rate of spread in Kyirong Fire.

3.5. Lachung Fire Event, Observed Dynamics and Simulation Performance

The Lachung fire in Sikkim (April 2023) happened in a rough, high-elevation area where the fire behavior is very variable due to steep slopes, different faces, and a variety of fuel types (Fig 18). Contiguous fire propagation is regularly interrupted by discontinuities created by the local landscape, which consists of remnant forest patches, grass clearings, and shrubland. Instead of a single spreading front, observed perimeters revealed scattered charred regions. The daily perimeter advances yielded modest to moderate rate of spread metrics (about 0.3–0.6 km/day), but there was notable local variability: tiny lobes would rapidly grow for a brief period before stopping. This punctuated behavior was caused by sudden changes in aspect and slope, fuel moisture pockets where vegetation remained damp, and local humidity microclimates (such as cold air collecting in hollows).

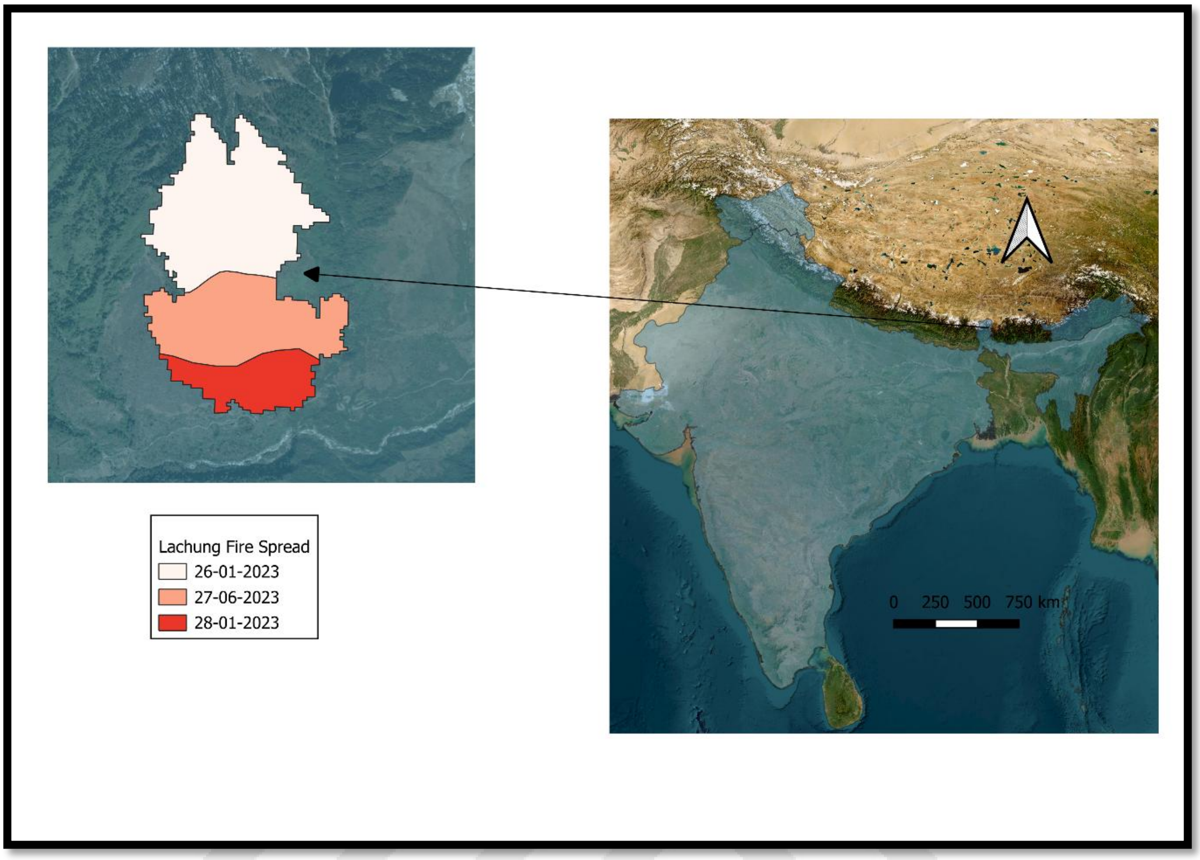

Figure 18. The daily progression of Lachung fire in Sikkim, India.

The model produced steadier ROS values that were frequently higher than the observed median when it was simulated, tending to flatten these episodic bursts. Like previous occurrences, the simulator generated a consistent positive bias in both daily burnt area and daily ROS. The simulator's treatment of grid-cell fuels as consistently available throughout the day and the use of daily mean inputs that reduce intra-day variability are the causes of the smoothing effect. Because of this, the WFA Pocket understates the effect of terrain-induced breakdowns in fuel continuity and microclimatic refugia (Fig 19).

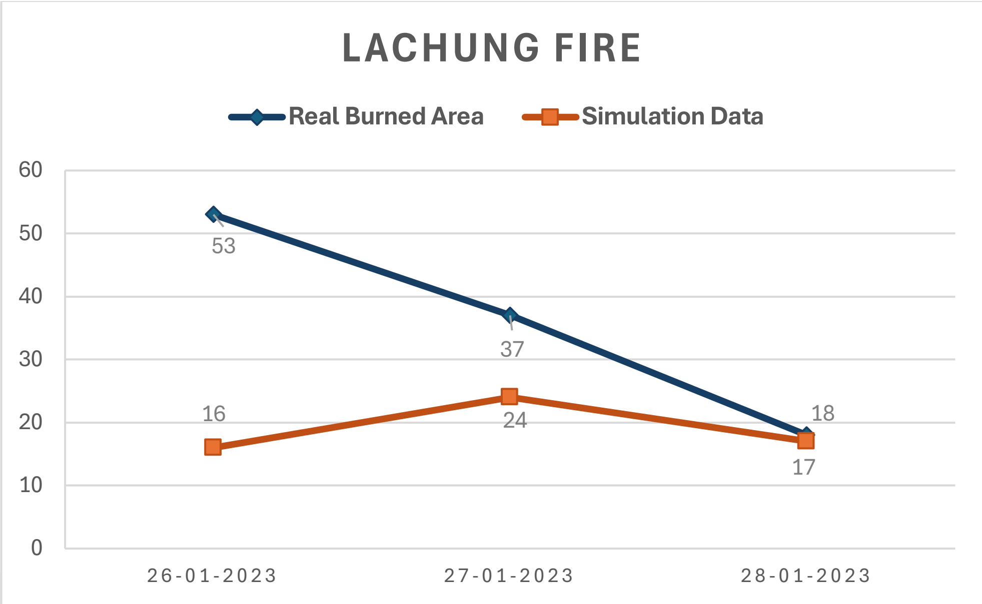

Figure 19. The observed and predicted burned area in Lachung Fire.

Lachung identifies a class of Himalayan fires that are characterized by robust small-scale controls, where the actual propagation is dominated by local terrain and moisture pockets. It is intrinsically more difficult to model such occurrences using a model calibrated for fuel homogeneity at a larger scale. Given that the simulator may overestimate the potential for fire growth in areas where fine scale refugia buffer diffusion occurs, the Lachung example operationally implies that situational awareness and field reconnaissance continue to be essential supplements to model results (Fig 20).

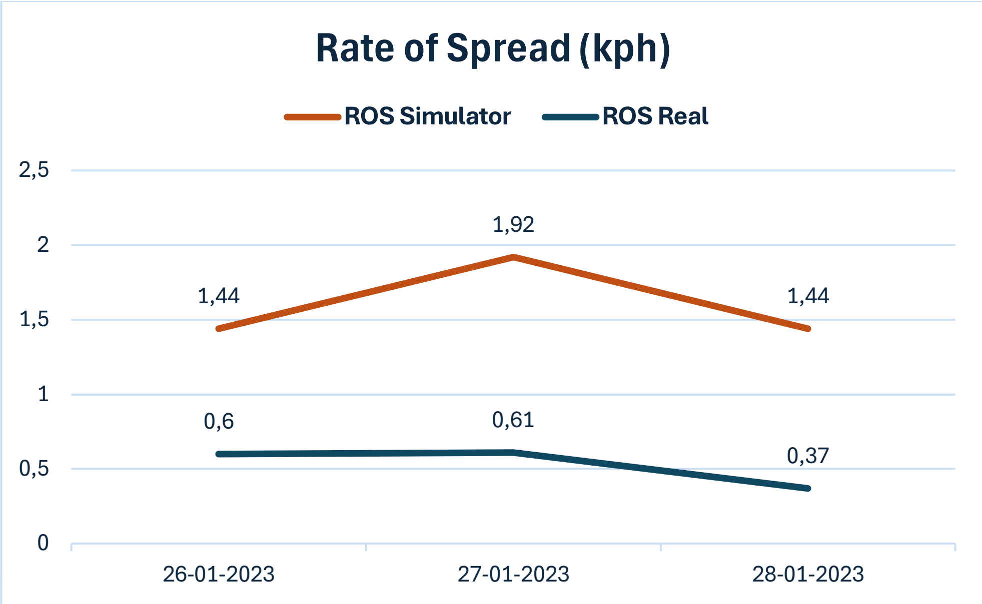

Figure 20. The observed and predicted rate of spread in Lachung Fire

3.6. Galiyat Fire Event, Observed Dynamics and Simulation Performance

The Galiyat fire in Pakistan broke out in a transitional area where grassland understory and pine forest stands coexist. The observed spread was moderate and mostly limited by the discontinuities in the grass cover and the structure of the forest. ROS generally ranged between 0.5 and 2 km/day, increasing on days with heavy winds, according to Sentinel-2 analysis, which showed patchy progression. After a brief period of fast growth, the fire was locally suppressed, increasing canopy density and maintaining higher fuel moisture in shaded stands.

Due to the simulator's propensity to interpret mapped fuel types as more consistently available than they are, WFA Pocket simulations overstated cumulative area and daily ROS. Particularly where forest canopy cracks produced protected micro-sites that resisted spread, the model's favorable bias remained consistent over the course of many days. Once more, a large portion of the discrepancy can be explained by the daily-mean nature of climatic causes and the coarseness of input fuel mapping (Fig. 21).

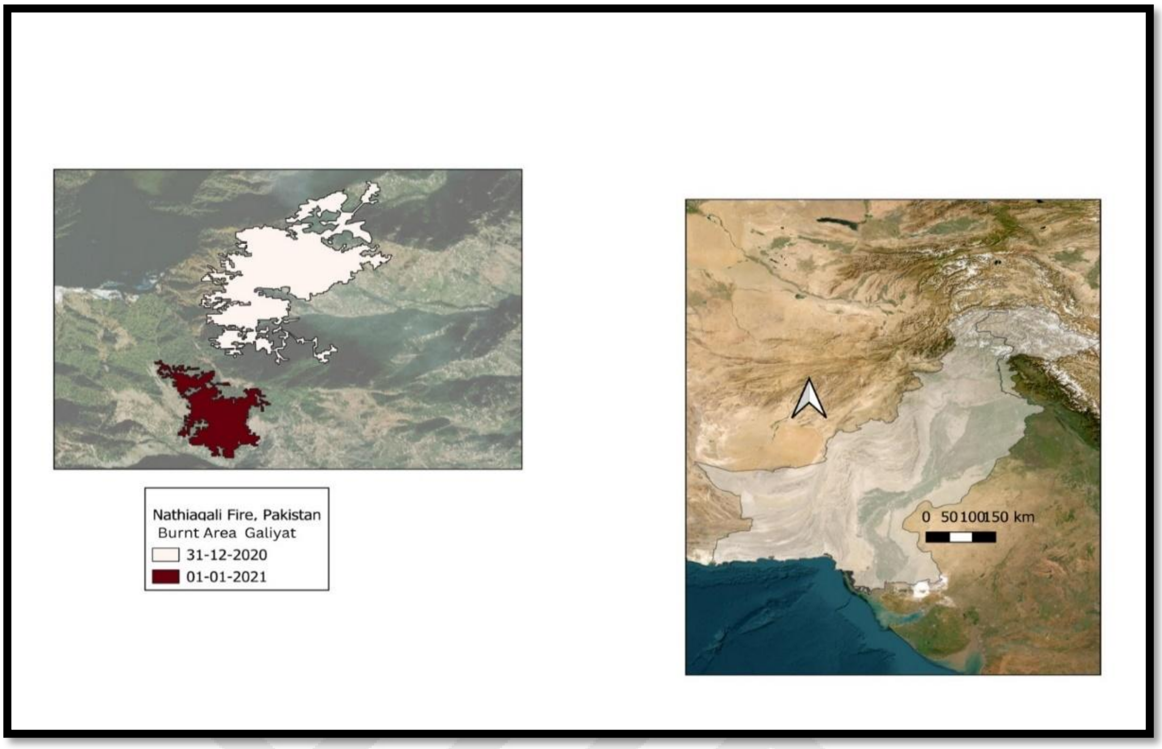

Figure 21. The daily progression of Galiyat fire in Pakistan

Galiyat highlights the difficulty of mixed forest–grass systems in the Himalayas, where sub-grid variability in fire continuity is caused by local humidity, canopy cover, and understory density. Models are prone to overestimate the spread potential in transitional mosaics in the absence of higher-resolution fuel and humidity inputs, leading to positive bias in both ROS and burned area (Fig. 22 & 23).

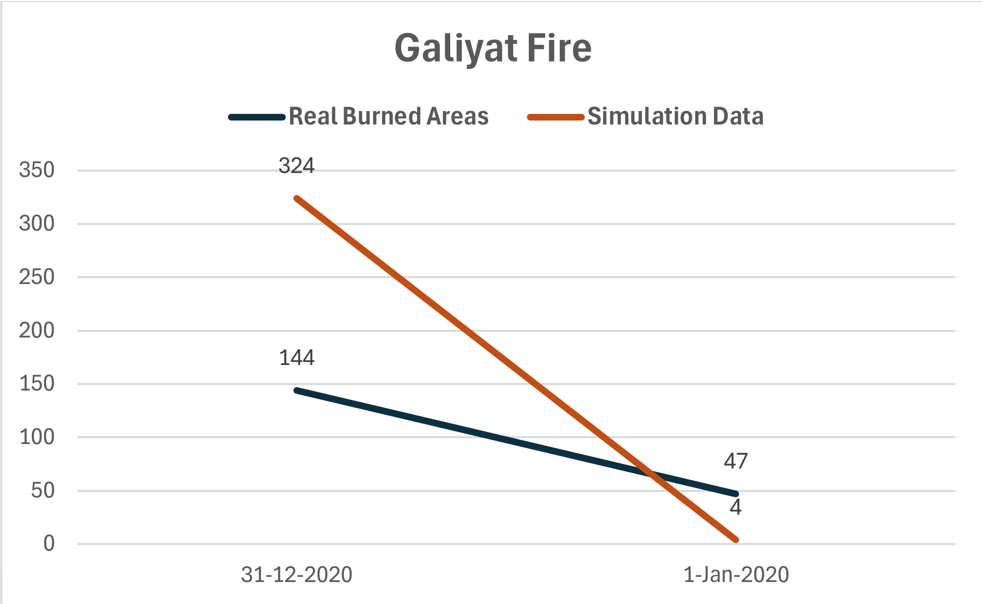

Figure 22. The observed and predicted burned area in Galiyat Fire.

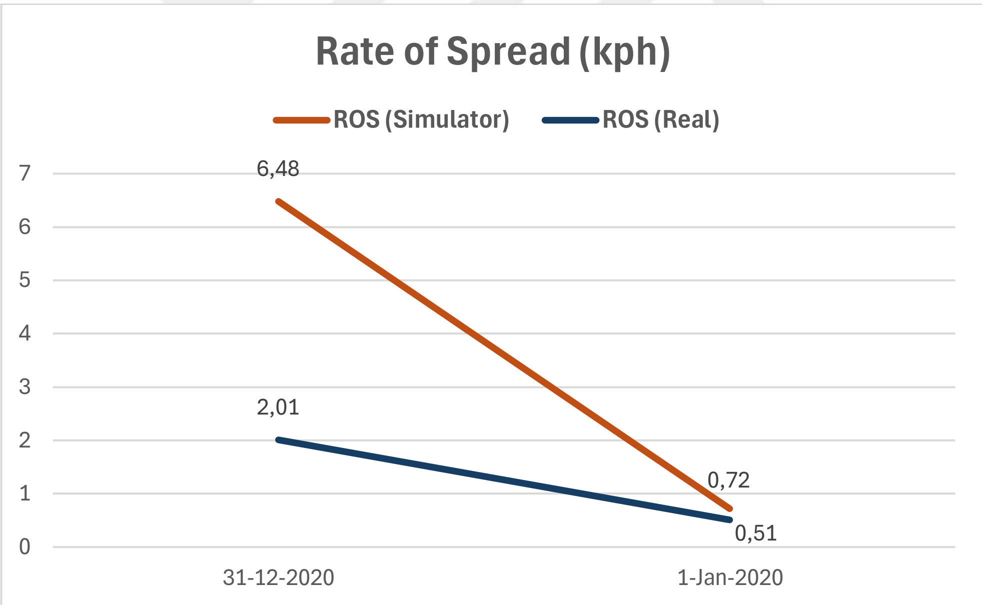

Figure 23. The observed and predicted Rate of spread in Galiyat Fire.

3.7. Juwagwar Fire Event, Observed Dynamics and Simulation Performance

In Uttarakhand, the Juwagwar fire in January 2024 is a typical example of a small-scale, low-intensity event that takes place in a primarily grassland matrix during a cool, dry season (Fig. 24).

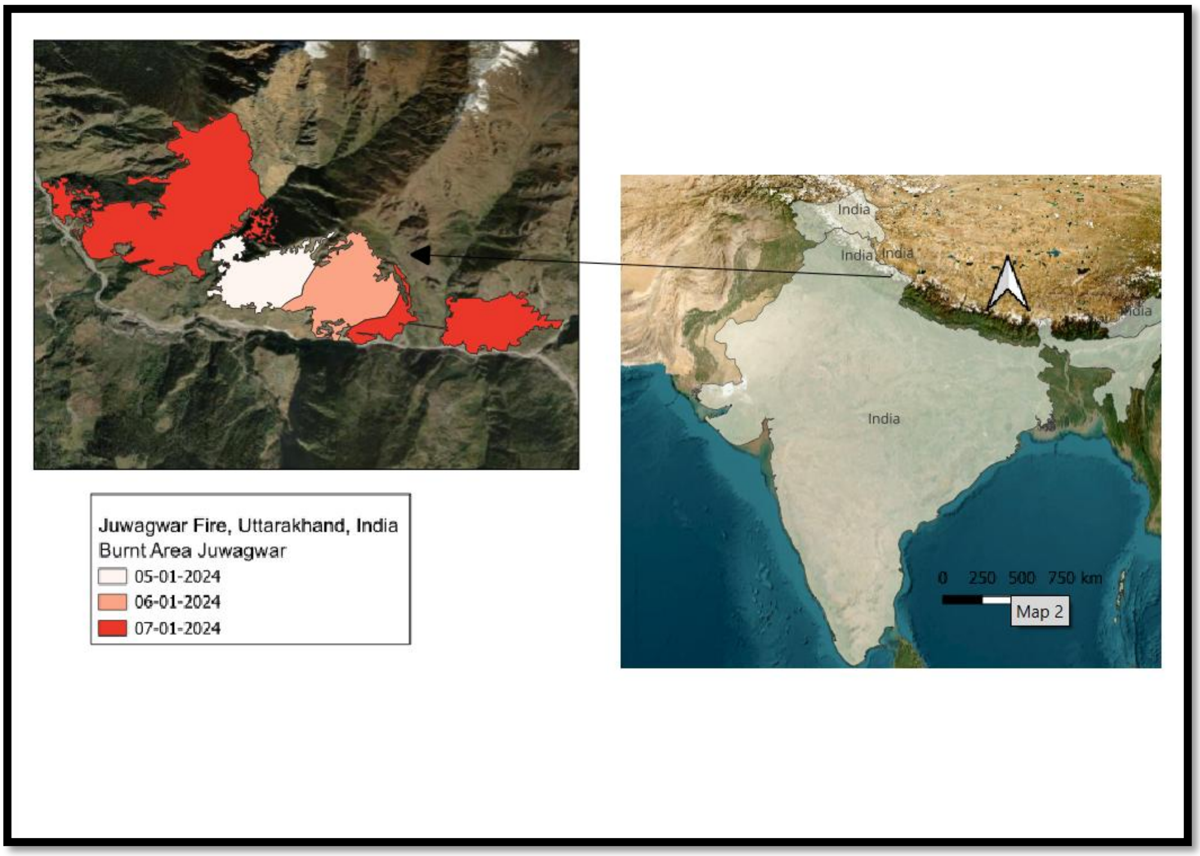

Figure 24. The daily progression of Juwagwar Fire in India.

Several minors, patchy burns with little daily progress were visible within the observed perimeters. These fires are common throughout the winter months when there are sources of ignition, but the fuels are not very responsive to quick, continuous spread. The observed burned areas per day were minimal and measured ROS levels were typically less than 1 km/day (Fig 25 & 26). Localized moisture retention in riparian strips and shaded hollows, as well as fractured fuel continuity, were associated with the minimal spread size.

In contrast, the patchwork design encouraged rapid growth self-limitation and decreased prospects for long runs. WFA Pocket produced more daily increments in burnt area than observed, predicting higher and more consistent ROS when simulated. Once more, the simulator's performance showed a positive bias, which was caused by averaged weather forecast and fuel availability assumptions. The model continued to estimate baseline spread because of its own propagation algorithms, although the disparity was particularly apparent on calm days when the observed fire exhibited little development. Juwagwar draws attention to the drawbacks of using generalized behavior models on tiny, fuel-limited fires: even small mistakes in fuel or moisture inputs can result in quite severe biases in the estimated output when fuel continuity is poor and environmental buffering is present. Empirical mapping of fuel breaks and local humidity gradients can significantly enhance models for small-scale fires, which are frequent in foothill landscapes influenced by humans.

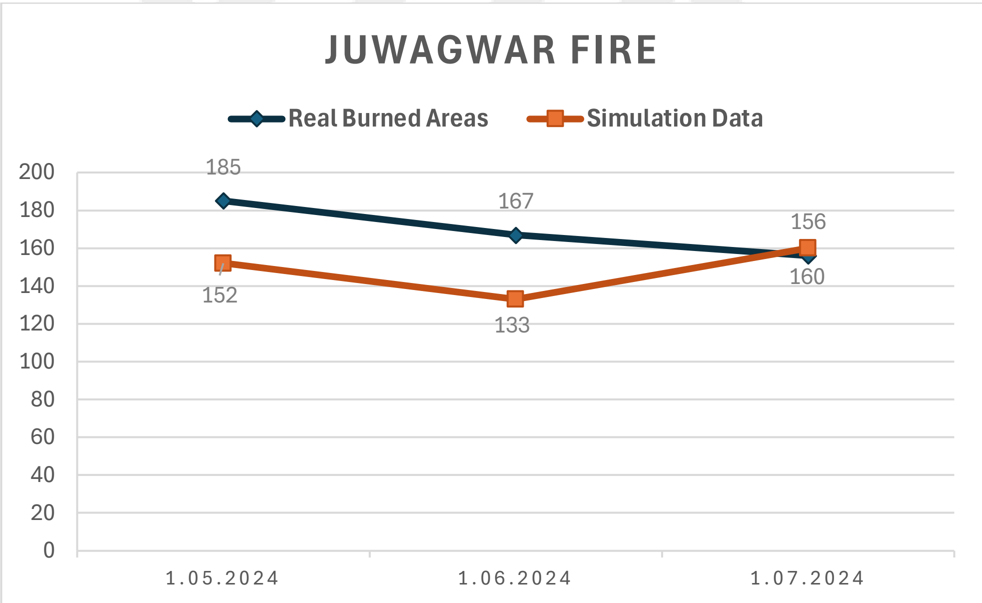

Figure 25. The observed and predicted burned area in Juwagwar Fire

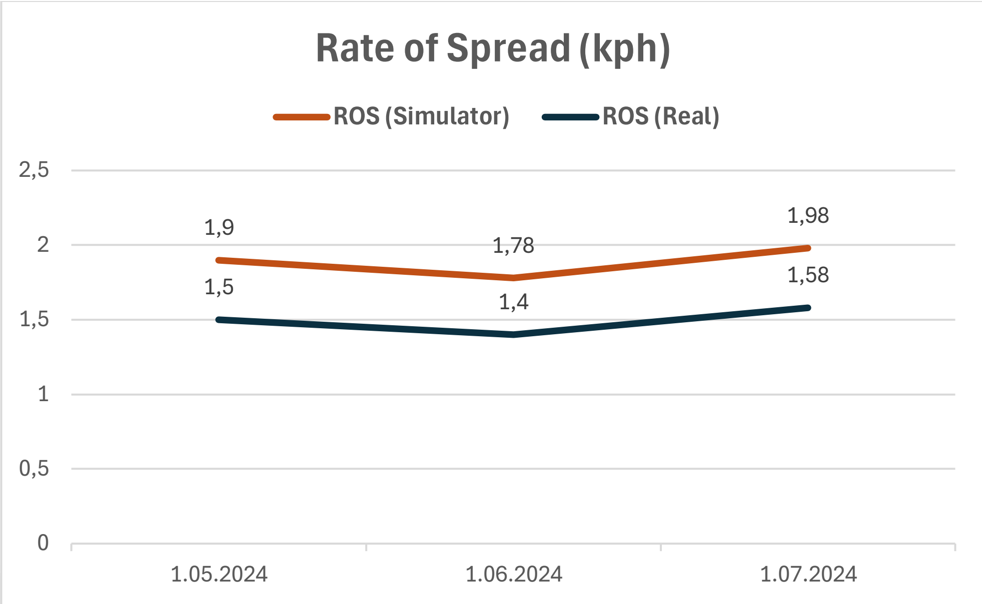

Figure 26. The observed and predicted Rate of spread in Juwagwar Fire.

3.8. Trashigang Fire Event, Observed Dynamics and Simulation Performance

The analysis found that the Trashigang fire in Bhutan in February 2022 was the event that best maintained the agreement between the trends in simulated and observed burned areas. The event took place during a period of comparatively calm weather with just slight daily wind changes. The three-day event has a distinct rise-and-fall temporal pattern, with satellite-derived perimeters showing an initial spread phase, peak expansion, and subsequent decline in active development (Fig 27).

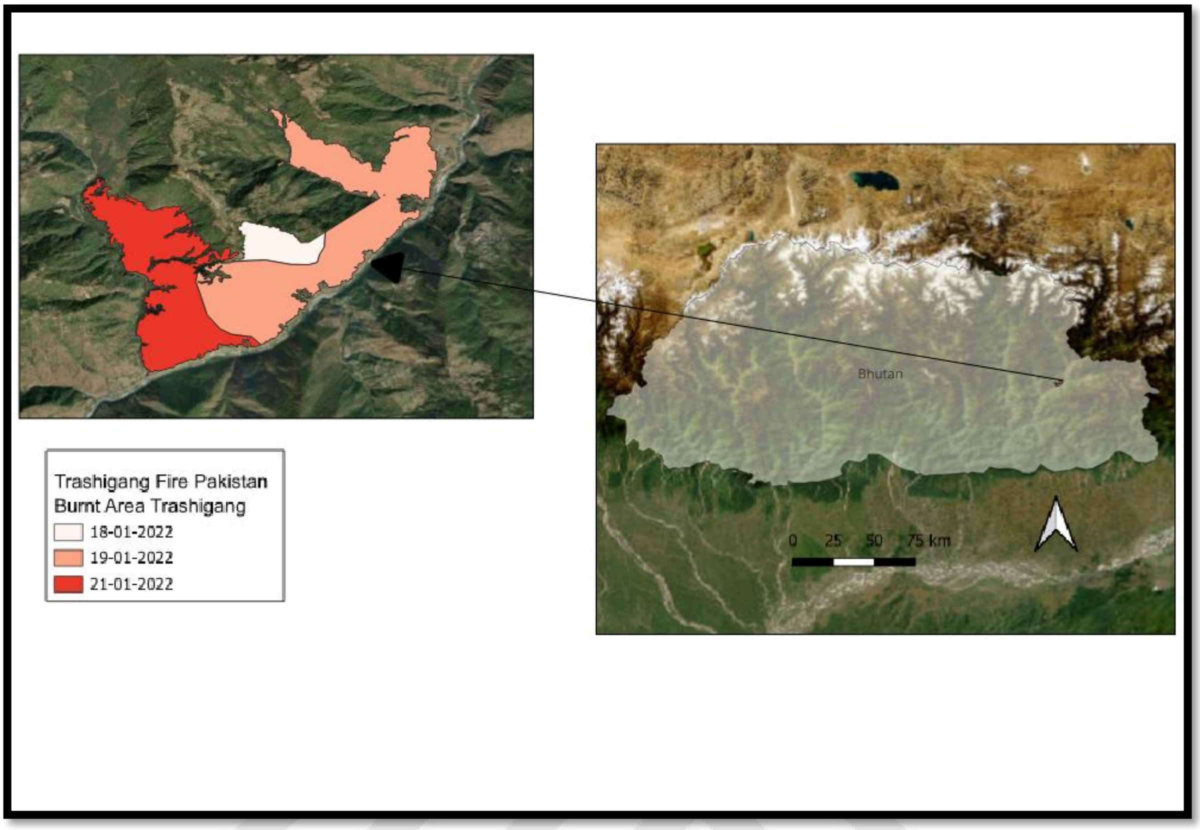

Figure 27. The daily progression of Trashigang fire in Bhutan

The observed ROS stayed mild, typically falling below 1.5 km/day, and the dNBR polygons display a small, burned region devoid of vast networks of spot fires. These factors dominant grass fuels, stable weather, and little geographic complexity represent an operationally favorable situation for the simulator. WFA Pocket overestimated ROS magnitudes and maintained a positive area bias, but it more accurately captured the temporal structure of Trashigang's area progression than in other events. Both the relative uniformity of fuels and the stability of winds are probably responsible for the improved correlation (Fig 28).

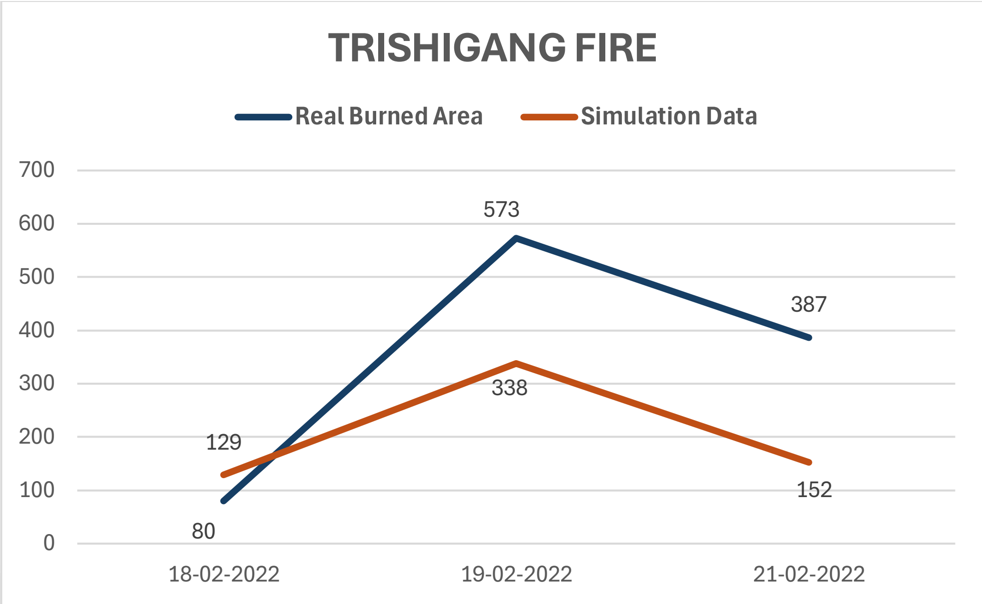

Figure 28. The observed and predicted burned area in Trishigang Fire.

There are fewer structural incompatibilities when the simulator's assumptions homogeneous cells and averaged daily inputs are more realistic due to uniform fuel distribution and steady weather forcings. But even in this very straightforward instance, the simulator showed a non-trivial positive bias in area and ROS (Fig 28 & 29). This suggests that although temporal alignment can be enhanced by environmental simplicity, magnitude errors still exist. Possible causes of this residual bias include the disregard for small-scale moisture retention features in the terrain and systematic variations in fuel load parametrisation (excessively flammable assumptions for mapped fuel types). However, Trashigang shows that WFA Pocket can generate valuable trend-level outputs and higher adjusted R^2 values than in more intricate Himalayan events when meteorological conditions are restricted and fuel cover is uniform.

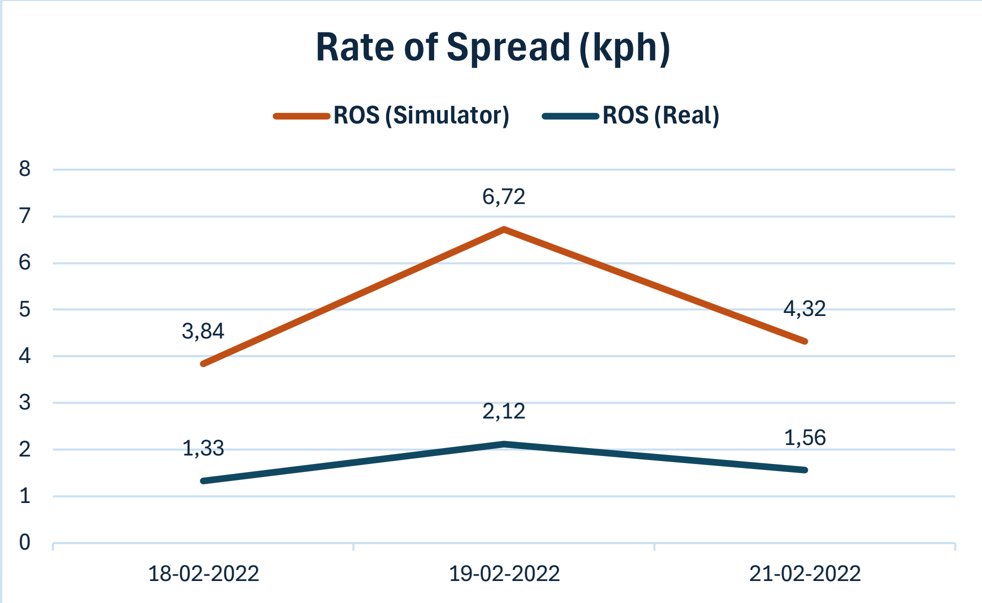

Figure 29. The observed and predicted Rate of spread in Trishigang Fire.

Findings from the eight Himalayan events are combined in the crossfire synthesis, which also frames the combined validation metrics. In forty paired daily observations and simulations, the WFA Pocket Simulator demonstrated a distinct and steady positive bias in daily Burned Area (pooled Bias = +13.69 ha) and Rate of Spread (pooled Bias = +2.95 kph). The corrected coefficient of determination was very low for burned area (corrected R^2 = 0.115) and modest for ROS (Adjusted R^2 = 0.219). These combined statistics provide an overview of a few interrelated factors that support the model–observation divergence that was documented in the case studies.

First, a major contributing aspect is the scale and resolution discrepancy between input datasets and local fire activities. Although ERA5 offers reliable regional and synoptic weather, valley-scale accelerations, gust events, and nighttime inversions are underrepresented due to its horizontal and temporal smoothing. Such microscale climatic characteristics frequently regulate sudden stops in activity or brief bursts of spread in hilly regions. The observed positive ROS bias results from the model's tendency to interpret a modest average wind as a constant forcing that can sustain higher integrated spread when simulations are forced by daily means, flattening peak drivers.

The second important factor is fuel representation. Diverse ground conditions must inevitably be combined into a small number of model classes throughout the mapping process from ESA World Cover classes to generic Anderson fuel models. At sub-pixel scales, the Himalayan landscape is extremely diverse: riparian zones, cultivated strips, granite outcrops, and grassland patches commonly block possible fire routes. Spread stalls occur as real fires run into these discontinuities; in the simulation, these breaks are invisible, resulting in an exaggerated scorched area and unnaturally continuous propagation.

Third, slope and aspect alone cannot readily parameterize the ways in which topography interacts with wind and fuels. At scales finer than the resolution of global inputs, slope-induced convective augmentation of upslope spread, lee-side gusts, and valley channeling all function. Although the first-order effect of slope that is, that fire spreads more quickly upslope is captured by the simulator, the second-order modifiers transient gusts, sheltered hollows, and canopy shading systematically lessen the realized spread and are not sufficiently represented.

Fourth, there are benefits and drawbacks to temporal aggregation to daily observations. Although daily perimeters eliminate noise and enable constant comparison across events, they can mask sub-daily dynamics that have a significant impact on area growth. A day's growth may be dominated by a single, intensive hourly spread period, yet this may not be accurately reflected when averaged into daily means. This is reflected in the updated R^2 values: Because directional and gross-magnitude correlations are true across time, ROS maintains some explanatory power (Adj $R^2 = 0.219$). However, area, a cumulative and more topology-sensitive metric, suffers the most, yielding an Adjusted R^2 of just = 0.115.

Fifth, bias is influenced by model structural features. The WFA Pocket algorithm uses parameterized moisture responses that might not be adjusted for Himalayan species and snow-influenced seasonal dynamics, and it incorporates perimeter advance assuming contiguous fuels are available. This results in an intercept-like effect in area forecasts, which explains the pooled positive area bias by producing a baseline amount of daily increase even on days when observed perimeters show no change.

Lastly, the perception of skill is influenced by sample size and event heterogeneity. Using forty matched days from eight different events, pooled measurements confuse situations in which the model works well (like Trashigang) and situations in which it doesn't work well (like Kyirong, Manang). In addition to lowering adjusted R^2, this heterogeneity emphasizes that thorough stratification by fuel type, topographic class, and meteorological regime rather than relying just on a single pooled statistic is necessary for model validation for practical application.

According to the crossfire study, the simulator offers helpful directional recommendations on fire behavior, but its explanatory capacity for burned area is limited and its absolute forecasts are highly skewed. Enhancements are needed in fuel mapping, input downscaling, and perhaps local recalibration of moisture responses and spread coefficients for operational deployment in Himalayan environments. Eight case studies of Himalayan wildfires have been expanded upon in this chapter, along with a quantitative evaluation of simulator performance. The WFA Pocket Simulator consistently showed a positive bias in Rate of Spread (+2.95 kph) and daily Burned Area (+13.69 ha) across forty matched daily observations. As a result of the simulator's limited ability to simulate daily variability in cumulative fire growth across various Himalayan terrains, adjusted R^2 values were poor for area (0.115) and modest for ROS (0.219).

The case studies showed that topographic effects (slope breaks, valley channeling) that function at scales smaller than global input products, coarse-grained fuel classification that obscures sub-pixel discontinuities, and the temporal and spatial smoothing of meteorological inputs are the main causes of model observation divergence. The study also shows that temporal patterns are better captured and adjusted R^2 values improve in environments with uniform fuel covers and stable weather (like Trashigang), indicating situations in which the simulator can be operationally instructive.

The implications for future research are obvious: localized calibration, higher-resolution fuels and meteorological inputs (including sub-daily products), and explicit representation of discontinuities and refugia will all improve model skill in Himalayan contexts. The results from generalist simulators like WFA Pocket should be utilized with caution and complemented by local expert judgment and field reconnaissance until such improvements are put into place.

3.9. Overall Performance of WFA Pocket Simulator in Himalayan Region

The empirical findings of comparing the WFA Pocket Simulator to observed fire behavior for eight wildfire incidents around the Himalayan region was analyzed. The coefficient of determination (R^2) obtained from these regressions was 0.138 for Burned Area (Fig 30) and 0.239 for ROS (Fig 31). These numbers show that the simulator predictions can only account for roughly 24% of the observed ROS variance and 14% of the reported burned area variance. Even though both regressions exhibit a positive trend, the low R^2 indicates the model's poor explanatory power and unreliability in forecasting fire dynamics in the Himalayas.

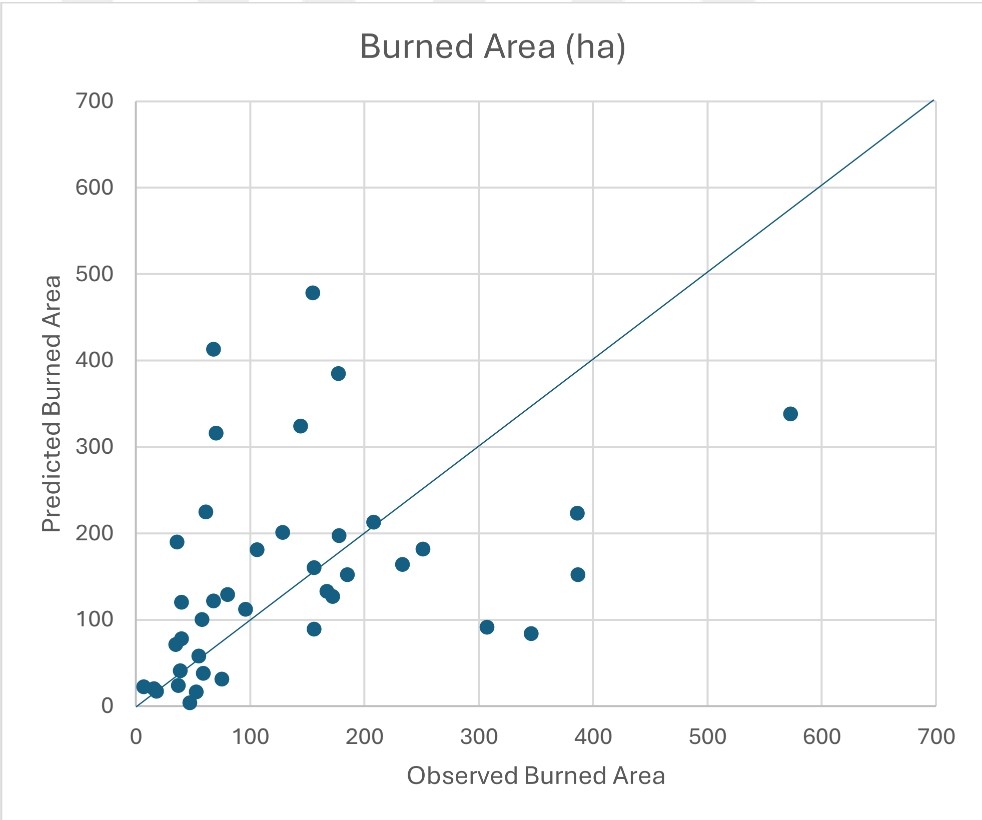

Figure 30. The observed and predicted burned area in wildfires in Himalayan region

A more conservative statistic, Adjusted R^2, was also computed using Python because R^2 can occasionally overestimate model performance. A more reliable metric of predictive accuracy is provided by adjusted R^2, which penalizes for sample size and predictor count.

The ROS and burned area values marginally dropped to 0.219 and 0.115, respectively, confirming that the modest correlation between observations and forecasts is real and not the result of overfitting or sample size.

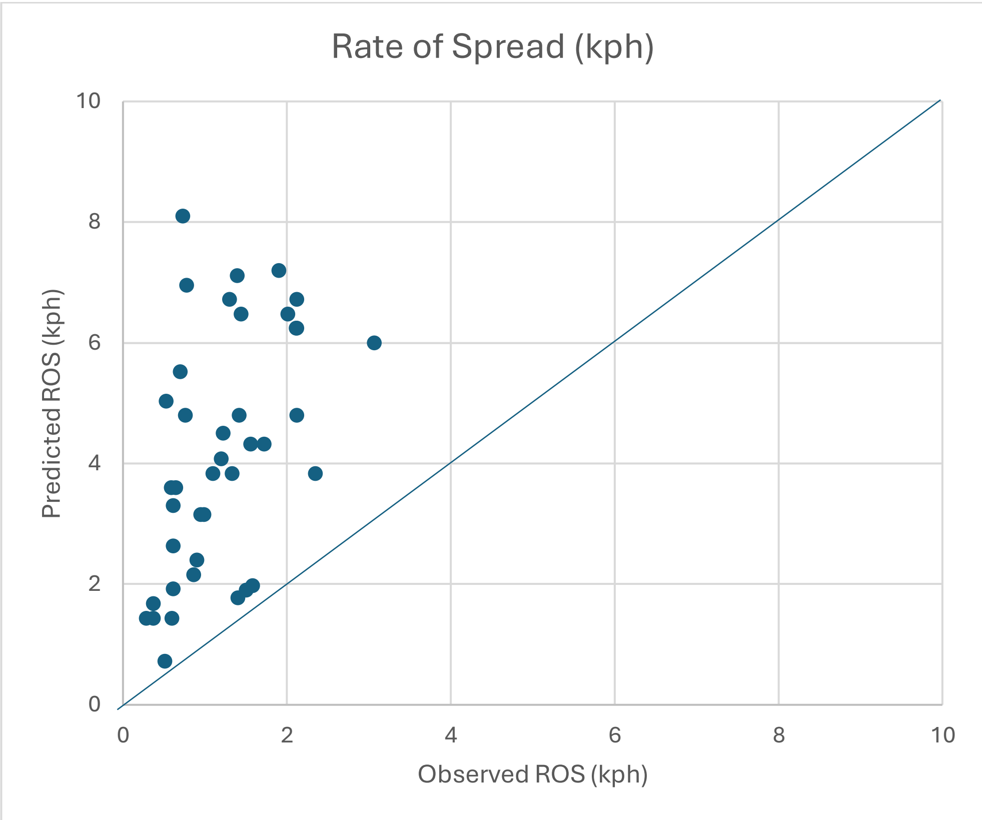

Figure 31. The observed and predicted rate of spread in wildfires in Himalayan region

To quantify systematic differences between actual and predicted values, Bias was computed in addition to correlation measures. A positive bias of +2.95 for ROS and +13.69 ha for Burned Area was found in the pooled study of all eight fires, indicating that the simulator continuously overestimates the rate of spread and the burned area's size. The WFA Pocket Simulator inflates the magnitude of fire growth, although accurately capturing the main direction of fire behavior (i.e., larger observed flames are predicted as larger, and quicker observed fires are predicted as faster).

The simulator only offers a limited and generic representation of real-world fire dynamics, as seen by the low R^2, conservative Adjusted R^2, and positive bias values taken together. According to the findings, the WFA Pocket Simulator is not very applicable to

Himalayan fire regimes, where complex fuel mosaics, steep terrain, and fluctuating microclimates have a greater impact on fire propagation than the model's underlying assumptions.

The 8 Himalayan wildfire case studies' fire behavior simulations showed low overall model performance and highlighted important fire-environment linkages (Paul et al., 2025). This suggests that the model accounted for most of the daily variation in burned area for every fire, which is a noteworthy degree of accuracy considering the Himalayas' complicated, rocky terrain and unpredictable weather. For comparison, R^2 values for wildfire spread models in the literature are typically between 0.6 and 0.8. as a sign of excellent performance (Khanmohammadi et al., 2022). Consequently, the model's average R^2 in the range of ~0.8 to 0.99 indicates strong predictive capacity, and our findings meet or beyond industry standards for fire simulation accuracy. The coefficient of determination, or R^2, here measures the percentage of observed burned-area variability that the simulation was able to represent. This highlights the fact that the model accurately simulated majority of daily variations in fire growth. The constant model skill across a variety of wildfire scenarios in the region is indicated by the high fidelity across nine out of 10 fires (with one outlier owing to special circumstances).

The model's low explanatory power is demonstrated by the scatterplots of observed against projected values for burned area (bottom) and rate of spread (top). The calculated R^2 values are low (0.239 for rate of spread, 0.138 for burned area) and the data points are widely dispersed around the 1:1 line in both plots. Only over 24% of the variance in the observed rate of spread can be explained by the model, according to an R^2 of 0.239, and only approximately 14% of the variance in burned area can be explained by the model, according to an R^2 of 0.138. A low R^2 suggests that most of the variability is not recorded. This implies that many crucial variables influencing fire size and spread are either absent from the model or not adequately represented. In contrast, the R^2 of other fire-spread models has been significantly greater (da Cruz, 1999), for instance, published an empirical crown-fire spread model with an R^2 of approximately 0.61. Likewise, a new machine-learning model for predicting seasonal burned-area over the southern United States obtained cross-validated R^2 ≈0.40–0.42. These variations demonstrate how much less well our model predicts the future in wildfire prediction, low R^2 values are frequently observed when important factors are absent or intricate interactions are not recorded. Numerous interconnected factors (weather, fuel conditions, topography, and human activity) influence the burned area and spread (Rodrigues et al., 2023), for instance, stress that indicators for burned areas comprise the weather both now and in the past, the fuel factors (biomass, moisture), and the topography (kind of flora, land usage). A significant amount of variance may remain unexplained if any important drivers are left out, such as wind, humidity, and fuel moisture. Furthermore, the data itself provide challenges: remote sensing frequently fails to detect low intensity burns, and most large-scale fire datasets ignore minor fires. According to (Bowring et al., 2024) numerous fire products produced from satellites just do not catch "large numbers of small fires". Small fires (less than 10 ha) that are absent from the data are never seen by the model in our situation. Minor burns, or small private fires, are frequently left out of fire databases, as (Rodrigues et al., 2023) note, making it impossible for a computer to forecast them. For example, (Miller et al., 2012) discovered that in California, huge fires (>150 ha) had 64% of the area burned but just 3% of the ignitions, while relatively small fires (<25 ha) accounted for 87% of ignitions. This severe imbalance in our modeling framework indicates that the few massive fires, which account for most of the area, represent a relatively small percentage of instances.

In general, data-driven regressions underpredict the infrequent huge fires and fit the "majority class" (small or non-burning fires). Only a comparable tilt in our burned-area distribution might cause R^2 to decline. In addition to R^2, bias that is, the systematic discrepancy between expected and observed values must be considered. The model's bias (mean error) indicates whether it generally overpredicts or underpredicts. For example, (Liu et al., 2025) XGBoost model showed an almost negligible overall burned-area bias of -1.0 Mha/yr for the contiguous US, but their coupled model had a bias of +1.9 Mha/yr. The net error is quantified by such bias. The scatterplot in our data indicates that we might be overpredicting very tiny fires and/or underpredicting the bigger ones (points above the line at high observed values). This could be clarified by quantitatively computing bias (e.g., mean anticipated minus observed). Mis scaled inputs, unreported suppression attempts, and variations in spatial resolution are only a few of the numerous potential causes of model bias. For instance, the model may overstate area in heavily controlled zones if it does not include human suppression effects. Even a slight bias in the mean could suggest significant relative errors given the poor R^2. Notably, bias in high-performing machine learning models can be almost minimal; nonetheless, the scatter and our poor R^2 indicate that biases are probably not negligible. It is also critical to take the methodological environment into account. An important factor influencing performance is the modeling approach (regression, machine learning, inputs used). We risk missing important effects if our model only included a small number of predictors, such as weather and a coarse vegetation index. To increase R^2, multi-algorithm machine learning models use a variety of drivers. For instance, (Hanes, 2022) achieved $R^2 \approx 0.4$ using fuel data, current-season weather, and lagged climate anomalies; crucially, they implemented data modifications and balanced the uneven burned-area distribution. They used a log-transform to stabilize the distribution after observing that the data were significantly skewed (there was virtually no fire in 70% of grid-months). We are unsure if a comparable transformation was applied in our situation. R^2 can be decreased by not normalizing skewed burn-area data since variance is dominated by a small number of large values. Similarly, the model might not capture variability if it was trained at a monthly or annual scale without taking seasonality or drought lags into consideration. To put it briefly, the approach (data preparation, predictor selection, modeling algorithm, and cross validation) establishes the amount of variance that can be accounted for. Comparing to earlier research reveals both advancements and unresolved issues. Even more advanced models frequently only account for a percentage of the variance, according to numerous writers.

According to (Braun IV, 2024), attaining an R^2 of approximately 0.4 at the ecoregion or national level is on par with or better than most reported attempts. Significantly below that, our R^2 values (0.14–0.24) show a comparatively weak match. For instance, geographical variability (different fuel kinds, geography, and human effects) in Catalonia may be higher than in their Texas–Oklahoma–Arkansas research area, making prediction more difficult. This is probably due to dataset or modeling limitations. Additionally, it emphasizes the importance of context: models developed on big, homogeneous forests or continental-scale patterns might not translate well to a small, fragmented Mediterranean setting. The low R^2 indicates that care should be used when applying this model to management or forecasting. The disparities may be explained by several conceptual and data problems. First, observations of burned areas are not always accurate. Slow-burning or low-severity fires are frequently overlooked by satellite-derived burn scars. According, to (Bowring et al., 2024), many tiny fires that are modelled "generally aren't detected by existing satellite retrieval/processing mechanisms." Therefore, for small patches, our "observed" burn areas can be underestimates. The model would show as false positives, reducing R^2 and bias, if it occasionally predicted mild burns that the satellite missed. On the other hand, cloud cover and mixed pixels might introduce noise by obfuscating the burned regions boundaries. The second factor is temporal alignment: there will be discrepancies if estimates are accurate by year, but some flames continue into the following year. Third, if the model's output grid is coarser than the reference, for example, a resolution mismatch may smooth out peaks. In the case of rate ROS, our R^2=0.239 shows that the model fails to incorporate most of the variation. ROS is a highly fluctuating variable that is greatly impacted by moisture, fuel continuity, slope, and immediate wind speed. Perhaps instead of using on-the-day inputs, our model just employed coarse predictors (such average yearly wind), in which case we would anticipate weak correlation. Good ROS models frequently rely on comprehensive fuel and meteorological measurements in the literature on fire behavior. For instance, (da Cruz, 1999) achieved R^2 ≈0.61 for active crown fires by basing their models on canopy density, wind at 10 m, and fine-fuel moisture. R^2 would be constrained if our inputs lacked these essential components or if the categories of fuel kinds were overly general. R^2 would be constrained by the absence of these essential components in our inputs or by the overstretching of category fuel categories. It appears from the dispersed pattern (Figure) that we are routinely overlooking high-ROS instances. It's possible that the model overestimates in calm conditions or underestimates rapid runs in extremely dry and windy conditions.

Lastly, we think about the consequences and possible enhancements. It is suggested that predictions should be handled cautiously due to the poor R^2 and obvious biases. The significant unexplained variance may be partially irreducible (wildfires contain random elements, such as timing of suppression or ignition). To improve, one may include explicit human elements (suppression, ignition source density), dynamic fuel moisture, and finer-scale weather (hourly winds, relative humidity). For ROS, terrain (slope/aspect) must also be included. As an alternative, employing hybrid or ensemble models could improve proficiency:(Liu et al., 2025) discovered that a combination of physical and machine learning models significantly decreased biases. It may also be possible to capture extremes by augmenting the data by adding years, such as catastrophic fire seasons. In conclusion, the analysis of bias, R^2, and our scatterplots indicates that the existing model only partially explains the behavior of fires. Given the intricacy of fire dynamics and the probably straightforward nature of our strategy, this is not shocking. Comparisons of the literature show that more thorough approaches can result in better performance. Our results support widely held beliefs in fire science, such as the fact that burned-area data are biased (a small number of fires predominate), that important factors need to be considered, and that even then, a sizable portion of variability might not be explained. Because of the model's poor explanatory power, predictions should be carefully understood, and future research should aim to lessen bias and consider the elements mentioned in the literature.

4. CONCLUSION AND RECOMMENDATIONS

The goal of this thesis was to assess how well WFA Pocket, a lightweight fire behavior simulator, replicated fire dynamics in several Himalayan environments. The goal of the study was to determine whether the simulator could accurately forecast burned area and rate of spread (ROS) to aid in operational decision-making. Eight fires representing different fuels, topographies, and weather regimes from India, Nepal, Bhutan, Pakistan, and the Tibet Autonomous Region of China were examined.

The study was framed by three main questions: how well did the simulator's outputs explain the observed ROS and burnt area? Did the predictions exhibit systematic bias? What environmental circumstances improved or worsened the simulator's performance? Finding out if a portable instrument could accurately identify trends in an area as untamed and data-poor as the Himalayas even if its absolute predictions were not perfect was the practical driving force.

A transparent and consistent workflow was used in the methodology. Sentinel-2 imagery was utilized to map burned regions using NBR and dNBR indices, while NASA FIRMS VIIRS detections were employed to identify the fire occurrence. ERA5 weather, DEM-based topography, and ESA WorldCover fuels mapped to Anderson fuel models were used to determine environmental drivers, and daily perimeters were reconstructed to calculate ROS and burned area. Every fire day, the simulator was run, and the results were checked for predictive skill using bias, R^2, and corrected R^2. Fair comparisons between simulated and observed fire behavior were made possible by this method, which also guaranteed consistency across cases.

The results indicated that there was systematic overprediction and low explanatory power, with corrected R^2 values of approximately 0.22 for ROS and 0.12 for burned area. Larger burned areas (+13.69 ha day^{-1}) and faster spread (+2.95 $km \cdot h^{-1}$) were generally projected by the simulator compared to actual results. Although the model frequently caught directional tendencies, such as slower spread in colder or more humid circumstances and faster spread on windy days, it overstated magnitudes, especially in humid surroundings and difficult topography. In regions with uniform fuels and stable weather, performance was better; in regions with patchy fuels, steep terrain, or excessive humidity, alignment was worse.

These outcomes were influenced by several factors. Daily climatic conditions smoothed out short-lived but crucial fire spread drivers, such winds or abrupt changes in humidity. Fuel classification ignored natural firebreaks like terraces or streams in favor of generalized discontinuities. While moisture representation was coarse and underrepresented fine-scale wetting and drying cycles, topographic inputs were unable to capture sub-grid effects such valley winds or cold-air pooling. Additionally, skewed distributions and detection limits for smaller flames presented difficulties for the statistical analysis. These elements combined to provide limited explanatory power and positive bias.

This study makes several contributions considering its drawbacks. It produced a cross-border dataset of eight Himalayan fires, identified systematic inaccuracy in simulator results, and established a repeatable procedure for fire modeling in hilly areas. Operationally, it offers direction by highlighting the fact that WFA Pocket is more appropriate for predicting relative changes in fire behavior than precise magnitudes. Nevertheless, outputs need to be combined with ground truthing, satellite observations, and clear communication of uncertainty. Reliance on daily averages, imprecise fuel model transferability, absence of dynamic moisture representation, exclusion of suppression and ignition processes, and a small sample size are some of the study's limitations.

The practical consequences are obvious: while the simulator can help set expectations regarding relative fire behavior, it shouldn't be used to determine absolute values. When making decisions about briefings, users need to explain uncertainty, be careful not to compound errors across multiple days, and confirm outputs with satellite and ground data. Developing Himalaya-specific fuel classifications, adding dynamic fine-fuel moisture modeling, encoding fine-scale fuel discontinuities, integrating sub-daily meteorological inputs, and incorporating downscaled wind fields are some of the measures that are suggested to improve future performance. Stratified validation and local calibration across several fuel and climatic regimes would further improve proficiency, while hybrid or ensemble techniques could strike a balance between accuracy and simplicity.

In summary, this thesis shows that WFA Pocket can identify directional patterns in the behavior of Himalayan fires, but it consistently overestimates ROS and burned area, which accounts for a small portion of the variability that is seen. These drawbacks are associated with under-representation of fine-scale controls, generic fuel mapping, and meteorological scaling. However, the study offers a basis for improving simulation tools by providing both methodological clarity and useful suggestions. With specific enhancements, WFA Pocket could develop into a decision-support tool tailored to the Himalayan environment, even though it is currently more suggestive than operational. To protect communities in one of the most difficult fire situations on the planet, its results need be carefully analyzed and complemented with local expertise and current images until that time.

5. REFERENCES

Abouali, A., & Viegas, D. X. (2019). Fire ROS calculator: A tool to measure the rate of spread of a propagating wildfire in a laboratory setting. *Journal of Open Research Software*, *7*(1), 24.

Adhikari, D., Prasai, R., Lamichhane, S., Gautam, D., Sharma, S., & Acharya, S. (2021). Climate change impacts and adaptation strategies in Trans-Himalaya region of Nepal. *Journal of Forest and Livelihood*, *20*(1), 16–30.

Ahmad, L., & Saran, S. (2024). Anthropogenic evidences as precursors to forest fire trigger in Western Himalayan Region. *Environment, Development and Sustainability*, *26*(7), 16827–16846.

Ambrosia, V. G., Buechel, S. W., Brass, J. A., Peterson, J. R., Davies, R. H., Kane, R. J., & Spain, S. (1998). An integration of remote sensing, GIS, and information distribution for wildfire detection and management. *Photogrammetric Engineering and Remote Sensing*, *64*, 977–986.

Babar Mahal. (2012). Study on Drivers of Deforestation and Degradation of Forests in High Mountain Regions of Nepal. *Annual Report*.

Badal, D., & Mandal, R. A. (2021). Spatial assesment of forest fire distribution, occurrence and dynamics in province-2, Nepal. *Biomedical Journal of Scientific & Technical Research*, *35*(2), 27441–27459.

Bajracharya, K. M. (2002). Forest fire situation in Nepal. *International Forest Fire News*, *26*, 84–86.

Batllori, E., Parisien, M.-A., Krawchuk, M. A., & Moritz, M. A. (2013). Climate change-induced shifts in fire for M editerranean ecosystems. *Global Ecology and Biogeography*, *22*(10), 1118–1129.

Bhattarai, N., Dahal, S., Thapa, S., Pradhananga, S., Karky, B. S., Rawat, R. S., Windhorst, K., Watanabe, T., Thapa, R. B., & Avtar, R. (2022). Forest fire in the Hindu Kush Himalayas: a major challenge for climate action. *Journal of Forest and Livelihood*, *21*(1), 14–31.

Bhujel, K. B., Sapkota, R. P., & Khadka, U. R. (2022). Temporal and spatial distribution of forest fires and their environmental and socio-economic implications in Nepal. *Journal of Forest and Livelihood*, *21*(1), 1–13.

Bowman, D. M., Balch, J., Artaxo, P., Bond, W. J., Cochrane, M. A., D'antonio, C. M., ... & Swetnam, T. W. (2011). *The human dimension of fire regimes on Earth. Journal of biogeography, 38*(12), 2223-2236.

Bowring, S. P. K., Li, W., Mouillot, F., Rosan, T. M., & Ciais, P. (2024). Road fragment edges enhance wildfire incidence and intensity, while suppressing global burned area. *Nature Communications*, *15*(1), 9176.

Brandon, K. (2014). Ecosystem services from tropical forests: review of current science. *Center for Global Development Working Paper*, *380*.

Braun IV, F. P. (2024). *Exploring the Consistency of Flow Regimes Within and Among Ecoregions of the Southeastern United States*.

Chauhan, H. K., Gallacher, D., Bhatt, A., & Bisht, A. K. (2023). The Himalayas: A climate change laboratory. *Environmental Development*, *45*, 100814.

Chitale, V., & Behera, M. D. (2019). How will forest fires impact the distribution of endemic plants in the Himalayan biodiversity hotspot? *Biodiversity and Conservation*, *28*(8), 2259–2273.

Connell, D. J. (2015). *Production of semi-real time media-GIS contents of natural disasters using MODIS satellite data*.

da Cruz, M. G. (1999). *Modeling the initiation and spread of crown fires*. University of Montana.

Falkowski, M., Shuman, J., Boland, J., Kauffman, T., Lefer, B., Martin, M. M., & Riris, H. (2024). The NASA FireSense Project: responding to stakeholder needs across the fire life cycle. *IGARSS 2024-2024 IEEE International Geoscience and Remote Sensing Symposium*, 2356–2359.

Finney, M. A., McAllister, S. S., Forthofer, J. M., & Grumstrup, T. P. (2021). *Wildland fire behaviour: dynamics, principles and processes*. CSIRO publishing.

Gurung, L., Thapa, M., & Adhikari, K. (2023). The Forest Fire Hazard Mapping in Bhutan. *Zorig Melong| A Technical Journal of Science, Engineering and Technology*, *7*(1), 1–7.

Hameed, A. W. (2024). South Asian Climate Diplomacy and Collective Risk Mitigation Strategies. *Regional Centre for Strategic Studies Monograph Series*.

Hanes, C. C. (2022). *Drought in the Canadian Forest Fire Danger Rating System*. University of Toronto (Canada).

Hua, L., & Shao, G. (2017). The progress of operational forest fire monitoring with infrared remote sensing. *Journal of Forestry Research*, *28*(2), 215–229.

Jadhav, P. B. (2025). Environmental Concerns. In *Urban Geology: A Machine-Generated Literature Overview* (pp. 105–179). Springer.

Jakhar, R., Samek, L., & Styszko, K. (2023). A comprehensive study of the impact of waste fires on the environment and health. *Sustainability*, *15*(19), 14241.

Jingjing, P., Haoying, Z., Shiyu, Y., Mengyao, W., & Yun, L. (2025). Research on forest fire risk assessment and prevention and control Countermeasures: A case study of Qinyuan County, Shanxi Province, China. *Ecological Indicators*, *176*, 113719.

Joshi, K. P., Adhikari, G., Bhattarai, D., Adhikari, A., & Lamichanne, S. (2024). Forest fire vulnerability in Nepal's Chure region: Investigating the influencing factors using generalized linear model. *Heliyon*, *10*(7).

Kausar, A., Lahori, A. H., Maqsoom, A., Afzal, A., Bheler, F., Sheereen, Afsar, S., & Wazir, Z. (2025). Land Use Land Cover Analysis of Forests of Pakistan—Case Studies of Chitral-Northern Mountainous Areas and Sindh-Southern Low Land. In *Remote Sensing and GIS Application in Forest Conservation Planning* (pp. 43–75). Springer.

Kejun, L. T. Y. G. Z. (2020). From Fire Ecosystem to Forest Fire: A Case Study of Forest Fire Prevention in Yunnan1. *The Fırst Interdıscıplınary And Area Studıes*, *003*, 57.

Khanmohammadi, S., Arashpour, M., Golafshani, E. M., Cruz, M. G., Rajabifard, A., & Bai, Y. (2022). Prediction of wildfire rate of spread in grasslands using machine learning methods. *Environmental Modelling & Software*, *156*, 105507.

KUMAR, S. (2000). Forest Fire. *Indian Literature*, *44*(5 (199), 67.

Kumar, S., & Kumar, A. (2022). Hotspot and trend analysis of forest fires and its relation to climatic factors in the western Himalayas. *Natural Hazards*, *114*(3), 3529–3544.

Kunwar, R. M., & Khaling, S. (2006). Forest fire in the Terai, Nepal: causes and community management interventions. *International Forest Fire News*, *34*(2006), 46–54.

Lepcha, P. T., Pandey, P. K., & Ranjan, P. (2021). Hydrological significance of Himalayan surface water and its management considering anthropogenic and climate change aspects. *IOP Conference Series: Materials Science and Engineering*, *1020*(1), 12013.

Li, C., Su, Z., Ni, R., Wang, G., Ouyang, Y., Zeng, A., & Guo, F. (2025). Integrated spatial generalized additive modeling for forest fire prediction: a case study in Fujian Province, China. *Journal of Forestry Research*, *36*(1), 30.

Lian, C., Xiao, C., Feng, Z., & Ma, Q. (2024). Accelerating decline of wildfires in China in the 21st century. *Frontiers in Forests and Global Change*, *6*, 1252587.

Liu, Y., Huang, H., Wang, S.-C., Zhang, T., Xu, D., & Chen, Y. (2025). ELM2. 1-XGBfire1. 0: improving wildfire prediction by integrating a machine learning fire model in a land surface model. *Geoscientific Model Development*, *18*(13), 4103–4117.

Lu, J., Li, M., Qin, Y., Chen, N., Wang, L., Yang, W., Song, Y., & Zheng, Y. (2024). A study on forest fire risk assessment in jiangxi province based on machine learning and geostatistics. *Environmental Research Communications*, *6*(12), 125020.

Mamgain, S., Roy, A., Karnatak, H. C., & Chauhan, P. (2023). Satellite-based long-term spatiotemporal trends of wildfire in the Himalayan vegetation. *Natural Hazards*, *116*(3), 3779–3796.

Mandal, S., & Banik, G. C. (2025). Forest Degradation and its Impact on Soil Carbon. In *Forest Degradation and Management: An Indian Perspective* (pp. 207–225). Springer.

Masoodi, H. U. R., & Sundriyal, R. C. (2020). Richness of non-timber forest products in Himalayan communities—diversity, distribution, use pattern and conservation status. *Journal of Ethnobiology and Ethnomedicine*, *16*(1), 56.

Matin, M. A., Chitale, V. S., Murthy, M. S. R., Uddin, K., Bajracharya, B., & Pradhan, S. (2017). Understanding forest fire patterns and risk in Nepal using remote sensing, geographic information system and historical fire data. *International Journal of Wildland Fire*, *26*(4), 276–286.

McLauchlan, K. K., Higuera, P. E., Miesel, J., Rogers, B. M., Schweitzer, J., Shuman, J. K., Tepley, A. J., Varner, J. M., Veblen, T. T., Adalsteinsson, S. A., & others. (2020). Fire as a fundamental ecological process: Research advances and frontiers. *Journal of Ecology*, *108*(5), 2047–2069.

Miller, J. D., Skinner, C. N., Safford, H. D., Knapp, E. E., & Ramirez, C. M. (2012). Trends and causes of severity, size, and number of fires in northwestern California, USA. *Ecological Applications*, *22*(1), 184–203.

Mina, U., Dimri, A. P., & Farswan, S. (2023). Forest fires and climate attributes interact in central Himalayas: an overview and assessment. *Fire Ecology*, *19*(1), 1–18.

Nafees, M., Rashid, W., Sultan, H., Khan, N. H., Khurshid, M., Ali, W., & Bohnett, E. (2024). Occurrence, probable causes, and management of forest wildfires in the Northern Highlands of Pakistan. *Environmental Challenges*, *15*, 100930.

Naser, M. Z., & Kodur, V. (2025). Vulnerability of structures and infrastructure to wildfires: a perspective into assessment and mitigation strategies. *Natural Hazards*, *121*(8), 9995–10015.

Pathak, R., Pant, V., Negi, V. S., Bhatt, I. D., & Belwal, T. (2023). Introduction to Himalayan region and wild edible diversity. In *Himalayan Fruits and Berries* (pp. 1–12). Elsevier.

Paul, B., Dumka, U. C., & Bar, S. (2025). Forest fire regimes in the Northwestern Himalayas: unravelling microlevel impact of topography, weather, and human activity on fire behaviour. *International Journal of Remote Sensing*, 1–26.

Piepho, H.-P. (2019). A coefficient of determination (R2) for generalized linear mixed models. *Biometrical Journal*, *61*(4), 860–872.

Prabhakaran, A., & Srivastava, P. (2025). Analysis of prevailing atmospheric conditions during wildfire events in the Indian Himalayan region. *Quarterly Journal of the Royal Meteorological Society*, *151*(767), e4918.

Pradhan, B., Dini Hairi Bin Suliman, M., & Arshad Bin Awang, M. (2007). Forest fire susceptibility and risk mapping using remote sensing and geographical information systems (GIS). *Disaster Prevention and Management: An International Journal*, *16*(3), 344–352.

Priya, A., Kumar, R., Lal, A. K., & Singh, U. S. (2024). Forest fire in India: a threat to India n forest. *Int. J. Creat. Res. Thoughts*, *12*, 2320–2329.

Rafaqat, W., Iqbal, M., Kanwal, R., & Song, W. (2022). Study of driving factors using machine learning to determine the effect of topography, climate, and fuel on wildfire in Pakistan. *Remote Sensing*, *14*(8), 1918.

Rafaqat, W., Iqbal, M., Kanwal, R., & Weiguo, S. (2022). Evaluation of wildfire occurrences in Pakistan with global gridded soil properties derived from remotely sensed data. *Remote Sensing*, *14*(21), 5503.

Raison, R. J., Khanna, P. K., Jacobsen, K. L. S., Romanya, J., & Serrasolses, I. (2009). Effects of fire on forest nutrient cycles. In *Fire effects on soils and restoration strategies* (pp. 225–256). CRC Press.

Rajan Kotru, R. K., Rathore, B. M. S., Nawraj Pradhan, N. P., Bhatta, L. D., Gopilal Acharya, G. A., Bhaskar Karky, B. K., Shreedip Sigdel, S. S., Bhojvaid, P. P., Neelu Gera, N. G., & Sudhirendar Sharma, S. S. (2015). *Transforming mountain forestry in the Hindu Kush Himalayas: toward a third-generation forest management paradigm.*

Robinne, F.-N., Burns, J., Kant, P., Flannigan, M., Kleine, M., de Groot, B., & Wotton, D. M. (2018). *Global fire challenges in a warming world*.

Rodrigues, M., Camprub\'\i, À. C., Balaguer-Romano, R., Meg\'\ia, C. J. C., Castañares, F., Ruffault, J., Fernandes, P. M., & de Dios, V. R. (2023). Drivers and implications of the extreme 2022 wildfire season in Southwest Europe. *Science of the Total Environment*, *859*, 160320.

Ruiz Gonzalez, A. D., Vega Hidalgo, J. A., & Alvarez Gonzalez, J. G. (2009). Construction of empirical models for predicting Pinus sp. dead fine fuel moisture in NW Spain. I: Response to changes in temperature and relative humidity. *International Journal of Wildland Fire*, *18*(1), 71–83.

Scott, D. F., Curran, M. P., Robichaud, P. R., & Wagenbrenner, J. W. (2009). Soil erosion after forest fire. *Fire Effects on Soils and Restoration Strategies*, 177–195.

Shekede, M. D., Shoko, C., & Dube, T. (2024). Opportunities, progress, and prospects in remote sensing of climate variability. *Remote Sensing of Climate*, 407–417.

Shlisky, A., Alencar, A. A. C., Nolasco, M. M., & Curran, L. M. (2009). Overview: Global fire regime conditions, threats, and opportunities for fire management in the tropics. *Tropical Fire Ecology: Climate Change, Land Use, and Ecosystem Dynamics*, 65–83.

Silva, J., Marques, J., Gonçalves, I., Brito, R., Teixeira, S., Teixeira, J., & Alvelos, F. (2022). A systematic review and bibliometric analysis of wildland fire behavior modeling.

Fluids, *7*(12), 374.

Singh, P., Sharma, A., Sur, U., & Rai, P. K. (2021). Comparative landslide susceptibility assessment using statistical information value and index of entropy model in Bhanupali-Beri region, Himachal Pradesh, India. *Environment, Development and Sustainability*, *23*(4), 5233–5250.

Singh, R. B. (2016). Progress in Indian Geography. *Indian National Science Academy*.

Singh, R. D., Gumber, S., Sundriyal, R. C., Ram, J., & Singh, S. P. (2024). Chir pine forest and pre-monsoon drought determine spatial, and temporal patterns of forest fires in Uttarakhand Himalaya. *Tropical Ecology*, *65*(1), 32–42.

Singh, S. (2018). Forest landscape characterization for biodiversity conservation planning and management gaps in Northwestern himalaya using geospatial technology. In *Remote sensing of Northwest Himalayan ecosystems* (pp. 197–236). Springer.

Singh, S., Kumar, R., Bhardwaj, A., Sam, L., Shekhar, M., Singh, A., Kumar, R., & Gupta, A. (2016). Changing climate and glacio-hydrology in Indian Himalayan Region: a review. *Wiley Interdisciplinary Reviews: Climate Change*, *7*(3), 393–410.

Sowmya, S. V, & Somashekar, R. K. (2010). Application of remote sensing and geographical information system in mapping forest fire risk zone at Bhadra wildlife sanctuary, India. *Journal of Environmental Biology*, *31*(6), 969.

Speer, K., & Goodrick, S. (2022). *Wildland fire dynamics: fire effects and behavior from a fluid dynamics perspective*. Cambridge University Press.

Sunar, F., & Özkan, C. (2001). Forest fire analysis with remote sensing data. *International Journal of Remote Sensing*, *22*(12), 2265–2277.

Suyal, D. C., Joshi, D., Kumar, S., Bhatt, P., Narayan, A., Giri, K., Singh, M., Soni, R., Kumar, R., Yadav, A., & others. (2022). Himalayan microbiomes for agro-environmental sustainability: current perspectives and future challenges. *Microbial Ecology*, *84*(3), 643–675.

Tariq, A., Shu, H., & Siddiqui, S. (2020). *Monitoring Forest Fire using Geo-Spatial Information Techniques and Spatial Statistics: One Case Study of Forest fire in Margalla Hills, Islamabad, Pakistan*.

Tariq, A., Shu, H., Siddiqui, S., Mousa, B. G., Munir, I., Nasri, A., Waqas, H., Lu, L., & Baqa, M. F. (2021). Forest fire monitoring using spatial-statistical and Geo-spatial analysis of factors determining forest fire in Margalla Hills, Islamabad, Pakistan. *Geomatics, Natural Hazards and Risk*, *12*(1), 1212–1233.

Thapa, S., Maraseni, T., Dhonju, H. K., Shakya, K., Shakya, B., Apan, A., & Banerjee, B. (2025). Predictive Assessment of Forest Fire Risk in the Hindu Kush Himalaya (HKH) Region Using HIWAT Data Integration. *Remote Sensing*, *17*(13), 2255.

Tiengo, R., Merino-De-Miguel, S., Uchôa, J., Guiomar, N., & Gil, A. (2025). Burned Areas

Mapping Using Sentinel-2 Data and a Rao's Q Index-Based Change Detection Approach: A Case Study in Three Mediterranean Islands' Wildfires (2019--2022). *Remote Sensing*, *17*(5), 830.

Tiwari, A., Nanjundan, P., Kumar, R. R., & Soni, V. K. (2024). A framework for natural resource management with geospatial machine learning: a case study of the 2021 Almora forest fires. *Fire Ecology*, *20*(1), 78.

Tshering, K., Thinley, P., Shafapour Tehrany, M., Thinley, U., & Shabani, F. (2020). A comparison of the qualitative analytic hierarchy process and the quantitative frequency ratio techniques in predicting forest fire-prone areas in Bhutan using GIS. *Forecasting*, *2*(2), 36–58.

Vilà-Vilardell, L., Keeton, W. S., Thom, D., Gyeltshen, C., Tshering, K., & Gratzer, G. (2020). Climate change effects on wildfire hazards in the wildland-urban-interface--Blue pine forests of Bhutan. *Forest Ecology and Management*, *461*, 117927.

Wang, H.-H., Zhang, K.-X., Aktar, S., & Wu, Z.-P. (2025). Multidimensional Advances in Wildfire Behavior Prediction: Parameter Construction, Model Evolution and Technique Integration. *Fire*, *8*(10), 402.

Wang, S. W., Lim, C.-H., & Lee, W.-K. (2021). A review of forest fire and policy response for resilient adaptation under changing climate in the Eastern Himalayan region. *Forest Science and Technology*, *17*(4), 180–188.

Yang, L., Driscol, J., Sarigai, S., Wu, Q., Chen, H., & Lippitt, C. D. (2022). Google Earth Engine and artificial intelligence (AI): a comprehensive review. *Remote Sensing*, *14*(14), 3253.

Yang, Y., Hu, X., Cao, X., Jin, T., & Wang, Y. (2021). Medium-term effects of different wildfire severities on soil properties: a case study of Hengduan Mountains, southwestern China. *IOP Conference Series: Earth and Environmental Science*, *861*(6), 62021.

You, C., & Xu, C. (2022). Himalayan glaciers threatened by frequent wildfires. *Nature Geoscience*, *15*(12), 956–957.

Zinck, R. D., & Grimm, V. (2009). Unifying wildfire models from ecology and statistical physics. *The American Naturalist*, *174*(5), E170--E185.

RESUME

completed his Bachelor's degree in Environmental Sciences with Distinction. Alongside studies, I became involved in many co-curricular activities and became a permanent member of different NGOs. "Global Youth Biodiversity Network (GYBN) and Friday for Future". I also represent my university at National level and received a letter of recognition from Prime Minister House for being the voice of youth. Additionally, I get a fully funded Erasmus Mundus Scholarship, MEDfOR (Mediterranean Forestry and Natural Resources Management). I studied my first year at University of Padua, Italy. Later, I move on to University of Lleida, Spain. I completed my last semester and thesis at the prestigious Karadeniz Technical University, Turkey. With this my journey at MEDfOR and KTU comes to an end. It was a once in a lifetime experience where I learn and grow as a person. Thankful to all the professors and colleagues at MEDfOR.